Spin determination of resonance structure in (^{235}U + n) below 25 keV*

M. S. Moore, J. D. Moses, and G. A. Keyworth
University of California, Los Alamos Scientific Laboratory, Los Alamos, New Mexico 87545

J. W. T. Dabbs and N. W. Hill
Oak Ridge National Laboratory, Oak Ridge, Tennessee 37830

(Received 11 October 1977; revised manuscript received 12 June 1978)

Measurements made with a polarized neutron beam and a polarized target of ^{235}U have been analyzed to obtain spin-separated fission cross sections of (^{235}U + n) below 25 keV neutron energy. Analysis of the cross section data in the resolved resonance region has been carried out to obtain a better estimate of average parameters than has been previously available. The average parameters have been used as the starting point for an extraction of energy-dependent average parameters in the unresolved resonance region. The results of this analysis show evidence for intermediate structure in the spin-4 component.

[NUCLEAR REACTIONS, FISSION ^{235}U(n,f), E=1 eV–25 keV; measured J dependence of $\sigma(E)$, deduced resonance parameters to 100 eV, spin assignments to 300 eV. Evidence for intermediate structure in $\langle \Gamma_f \rangle$.]

I. INTRODUCTION

The low-energy neutron-induced fission cross section of ^{235}U has perhaps been more extensively studied than that of any other nucleus, yet our understanding of the fission process in ^{235}U is far from complete. More than 20 years ago, it was realized that fission is a few-channel process, and that, in order to account correctly for the observed asymmetries in the fission resonances, a multilevel treatment is required. For several years it has been conjectured that many of the properties associated with fission, such as the fragment mass distribution, the fragment kinetic energy, the number of neutrons emitted, the γ-ray energy release, etc., should depend on the fission channels. The most important piece of information that has been lacking in such studies is a complete set of spin assignments for the observed resonance structure.

In the unresolved resonance region, the existence of pronounced fluctuations in the neutron-induced fission cross section of ^{235}U below ~100 keV is well established, and several analyses[1-4] have indicated that these fluctuations cannot be explained by the usual statistical model treatment of unresolved resonances. The only mechanism that is known to lead to intermediate structure in fission is modulation of the fission widths by states of the second well of a double-humped fission barrier, called class II states. Cao *et al.*[1] have concluded that the observed frequency of the fluctuations in the fission cross section of ^{235}U is consistent with the systematics of subthreshold fission for nonfissile targets and of second-well parameters deduced from fission isomers. This mechanism requires that each of the fluctuations be produced by class II states of definite spin. It has been experimentally verified by Keyworth *et al.*[5] for (^{237}Np + n) that each of the subbarrier fission clumps consists of fine structure resonances (class I states) which all have the same spin. One thus expects that if the structure in (^{235}U + n) arises from such a mechanism, the nonstatistical behavior in the fission cross section should also show a spin dependence.

The technique of using polarized neutrons on a polarized target of ^{235}U, as the definitive method of determining the spins of resonances in the compound nucleus ^{236}U, has been discussed by Keyworth *et al.*,[6,7] who reported spin assignments for many of the prominent resonances below 60 eV. The present paper gives the results of a more extensive determination of the resonance spins of (^{235}U + n), with increased polarization and greatly improved statistical accuracy. These data have been processed to obtain spin-separated fission cross sections for each of the two s-wave spin states. Unambiguous spin assignments could then be made for all the known resonances in (^{235}U + n) below 60 eV, and several previously unreported resonances have been observed. Spin assignments have been made for the prominent structure in (^{235}U + n) below 300 eV neutron energy, and clear evidence has been found for intermediate structure in the spin-4 component of the ^{235}U fission cross section in the unresolved region.

The next section of this paper describes briefly the experimental measurement and the method of data processing, including the error treatment. Section III contains the treatment of the resolved resonance region, and Sec. IV the extraction of average pa-

rameters. In Sec. V, the average parameters are used in an analysis of the unresolved resonance region in which energy-dependent average parameters are obtained below 25 keV. The results of this analysis are then used to address the question of a spin dependence of intermediate structure in (^{235}U+n) in this region.

II. EXPERIMENTAL MEASUREMENT AND DATA REDUCTION

The measurement was carried out on the Oak Ridge electron linear accelerator (ORELA) with an experimental arrangement identical to that previously described.[5-7] The neutron beam was polarized by transmission through $La_2Mg_3(NO_3)_{12}\cdot 24H_2O$ (LMN) in which the hydrogen in the water of hydration was polarized. The target was a polarized sample of ^{235}US. The data consisted of time-of-flight spectra of prompt fission neutrons emitted from the sample with the neutron beam polarized parallel and antiparallel to the polarization direction of the target, and of the transmitted neutron beam under the same conditions. Table I summarizes the experimental running conditions.

The neutron polarization was determined by monitoring the change in transmission observed with the LMN polarized and unpolarized before and after each run, according to the relationship[8]

$$f_n = \tanh(\cosh^{-1} T), \tag{1}$$

where f_n is the neutron polarization and T is the ratio of the count rate observed with the LMN target polarized to that with it unpolarized. The average neutron polarization was slightly higher for the spin-4 enhanced series of runs than for the spin-3 enhanced series. The absolute nuclear polarization was not monitored during the experiment; it was left as a free parameter to be determined from well-known isolated resonances as a part of the data reduction.

Below 25 keV neutron energy, only s- and p-wave neutrons are expected to contribute appreciably to the observed cross section. The data reduction was carried out by assuming that only s-waves contribute. If N_3 and N_4 are the spin-3-enhanced and spin-4-enhanced count rates, then one can write

$$N_3 = A_3\sigma_3\phi_3 + A_4\sigma_4\phi_3 \tag{2a}$$

and

$$N_4 = B_3\sigma_3\phi_4 + B_4\sigma_4\phi_4 , \tag{2b}$$

where σ_3 and σ_4 are the spin-3 and spin-4 fission cross sections, ϕ_3 and ϕ_4 are the spin-3-enhanced and spin-4-enhanced fluxes (which, because of resonance self-shielding, are not the same), and A_3, A_4, B_3, and B_4 are constants to be calculated from the neutron polarizations, the nuclear polarization, and the target spin. For s-wave neu-

TABLE I. Experimental conditions for the second series of runs at ORELA.

Flight path (approximate)	Fission detector: 13.40 m Transmission detector: 15.28 m
Moderator thickness	36.6 mm H_2O
Beam burst/second	1000
Beam power (time averaged)	60 kW
Beam burst width	35 ns
Sample temperature	0.01 K
Filter array	0.047-g/cm^2 ^{10}B, 0.064-cm Cd, 1.27-cm Pb changed to 0.047-g/cm^2 ^{10}B, 0.084-cm Cd, 2.54-cm Pb after the first of seven runs, and changed to 0.047-g/cm^2 ^{10}B, 0.168-cm Cd, 3.81-cm Pb after the fourth of seven runs
LMN thickness	3.5 g/cm^2
LMN area	10.6 cm^2
US target thickness	0.21 g/cm^2 at 50° or 0.27 g/cm^2 at 90°
US target area	4.7 cm^2 at 50° or 3.6 cm^2 at 90°
Neutron beam area (at US target)	~7 cm^2
Average neutron polarizations:	spin 3 enhanced runs: 0.501 spin 4 enhanced runs: 0.518
Average nuclear polarization:	0.18
Average data collection time:	35 h/run

trons,

$$A_3 = (1 + f_n f_N)\,, \tag{3a}$$

$$B_3 = (1 - f_n' f_N)\,, \tag{3b}$$

$$A_4 = \left(1 - \frac{I}{I+1} f_n f_N\right)\,, \tag{3c}$$

$$B_4 = \left(1 + \frac{I}{I+1} f_n' f_N\right)\,, \tag{3d}$$

where f_n' and f_n are the neutron polarizations parallel and antiparallel to the nuclear polarization vector, f_N is the nuclear polarization, and I is the target spin.

Equations (2a) and (2b) are solved for the quantities

$$\sigma_4 = (A_3 N_4/\phi_4 - B_3 N_3/\phi_3)\Big/(A_3 B_4 - B_3 A_4)\,, \tag{4a}$$

and

$$\sigma_3 = (B_4 N_3/\phi_3 - A_4 N_4/\phi_4)\Big/(A_3 B_4 - B_3 A_4)\,. \tag{4b}$$

The data reduction was carried out by means of the following: (1) a spin-3-enhanced and a spin-4-enhanced effective cross section, N_3/ϕ_3 and N_4/ϕ_4, were constructed by dividing each of the observed count rates by its flux as determined from the transmission monitor. The sample was not thin at the largest resonances (it had a thickness of 0.62×10^{21} atoms/cm^2 of ^{235}U). One would expect that, at the peaks of these large resonances, dividing by the transmitted flux would overcalculate the cross sections. (One should instead divide by the average flux incident upon a nucleus of ^{235}U in the target.) However, as shown in Table I, the ^{235}US target covered only half the neutron beam viewed by the transmission detector, so to first order the sample self-shielding with its accompanying flux depolarization was correctly taken into account. (2) Using Eq. (4), σ_3 and σ_4 were determined. (3) A small empirically-determined energy-dependent background, varying as $1/E$, was subtracted from both σ_3 and σ_4 to make the between-resonance fission cross section correspond to acceptable values at low energies. (4) The data were normalized by setting the integral, from 7.8 to 11.0 eV, of the sum σ_3 and σ_4 equal to 241.24 b eV, as recommended by Leonard.[9] (5) Finally, steps (3) and (4) were repeated until both the between-resonance cross sections and the normalized integral agreed within the measurement uncertainty.

As a consistency check, fission integrals from 7.4 eV to 20 keV were compared with the recently published measurements of Gwin *et al.*[10] As shown in Table II, the agreement is reasonably good ex-

TABLE II. Integrals of ^{235}U fission cross sections below 20 keV.

Energy range (eV) E_1	E_2	$\int_{E_2}^{E_1}\sigma_3 dE$ (b eV)	$\int_{E_2}^{E_1}\sigma_4 dE$ (b eV)	$\int_{E_2}^{E_1}(\sigma_3+\sigma_4)dE$ (b eV)	Ratio to the data of Gwin *et al.* (Ref. 10)
7.4–	10	27.9	194.6	222.5	1.026
10.0–	15	145.1	71.1	216.2	1.015
15.0–	20.5	59.9	256.7	316.6	1.018
20.5–	33	220.2	232.5	452.7	1.031
33.0–	41	214.1	270.2	484.3	1.003
41.0–	60	421.7	483.9	905.5	1.005
60.0–	100	546.4	404.9	951.3	1.009
100.0–	200	909	1 160	2 069	0.986
300.0–	400	591	704	1 295	1.015
400.0–	500	613	683	1 296	0.988
500.0–	600	458	911	1 369	0.934
600.0–	700	488	589	1 077	0.969
700.0–	800	391	645	1 036	0.967
800.0–	900	308	459	767	0.966
900.0–	1 000	362	346	708	0.972
1 000.0–	2 000	3 013	3 742	6 755	0.954
2 000.0–	3 000	2 020	2 114	4 134	0.804
3 000.0–	4 000	1 543	2 407	3 950	0.862
4 000.0–	5 000	1 852	2 064	3 917	0.960
5 000.0–	6 000	1 574	2 271	3 845	1.034
6 000.0–	7 000	1 560	1 585	3 145	1.001
7 000.0–	8 000	1 583	1 474	3 057	1.003
8 000.0–	9 000	1 232	1 735	2 967	1.030
9 000.0–	10 000	1 390	1 560	2 950	0.980
10 000.0–	20 000	10 980	14 212	25 192	1.024

cept between 2 and 4 keV, where these data are low. A comparison of the present data with a fine-bin average of the data of Gwin *et al.* suggests that the discrepancy is due to the incomplete removal of the effects of large resonances in ^{139}La. The collimation system was not tight enough to prevent a part of the neutron beam from streaming around the sides of the LMN target. While these neutrons did not strike the polarized sample of ^{235}U, they did strike the larger ^{6}Li-glass transmission detector. This gives an erroneously high determination of the effective neutron flux in the vicinity of strong ^{139}La resonances and a low apparent fission cross section.

Flight paths were not measured in this experiment, but were determined from the positions of known resonances in cadmium, lanthanum, and aluminum present in the beam and in the signal observed with the ^{6}Li-glass flux monitor. By far the largest number of these resonances are those of cadmium, so in essence the energy scale of the present measurement is that of Liou *et al.*[11] For the fission signal, the flight path was established by minimizing the fluctuations in the ratio of fission counts to ^{6}Li-glass counts near these large resonances; a mismatch in the energy scale shows up as an asymmetric enhancement and depression of the ratio about such a resonance.

The self-absorption of the ^{6}Li-glass detector was taken into account at low energies, but otherwise the efficiency of the glass was assumed to vary as $1/\sqrt{E}$ over the entire region below 25 keV. This introduces a small systematic error, <1% below 15 keV and ~3% at 25 keV, compared to the ^{6}Li(n,α) cross section evaluation of Hale.[12]

The uncertainty in the measurement is dominated by the statistical uncertainty in the fission count rate; in the spin-separated cross sections the statistical uncertainty is quite large because of the subtraction of two large numbers to obtain a small difference, as implied in Eq. (4). If all other sources of error are neglected, the relative uncertainties in σ_3 and σ_4 are given by

$$\frac{\delta\sigma_3}{\sigma_3} \simeq (A_3^2 N_4 + B_3^2 N_3)^{1/2} \Big/ (A_3 N_3 - B_3 N_4)\,, \qquad (5a)$$

and

$$\frac{\delta\sigma_4}{\sigma_4} \simeq (B_4^2 N_3 + A_4^2 N_4)^{1/2} \Big/ (B_4 N_3 - A_4 N_4)\,. \qquad (5b)$$

The statistical uncertainty of the sum $\sigma_3+\sigma_4$ is very much smaller than that of the spin-separated cross sections. From Eqs. (3) and (4) one notes that

$$\sigma_f = \sigma_3 + \sigma_4 = \left(\frac{N_3}{\phi_3} f_n' f_N + \frac{N_4}{\phi_4} f_n f_N\right) \Big/ (A_3 B_4 - B_3 A_4)\,, \qquad (6)$$

and because f_n and f_n' are very nearly equal,

$$\frac{\delta\sigma_f}{\sigma_f} \simeq (N_3 + N_4)^{-1/2}\,. \qquad (7)$$

It is important to emphasize that this method of extracting spin-separated cross sections introduces an anticorrelation of σ_3 and σ_4 that is entirely due to statistical fluctuations: Whenever N_3 or N_4 shows a large statistical variation, such a variation will appear, magnified, in both σ_3 and σ_4, and in opposite directions.

The energy range spanned by the fission detector extended below 1 eV, which permitted verification of the spin assignment of 4^- to the 1.14 eV resonance. However, the ^{6}Li-glass flux monitor recorded events only above 1.6 eV. In order to extract spin-separated fission cross sections between 1.0 and 1.6 eV the sum $\sigma_3+\sigma_4$ was normalized, point by point, to the known[13] fission cross section of $(^{235}\mathrm{U}+n)$ in this region, and the ratio σ_3/σ_4 was used to determine the spin-separated cross sections.

The spin-separated fission cross sections and their sum, with assigned uncertainties, as determined from this measurement, from 1.6 eV to 25 keV, are available from the National Nuclear Data Center (NNDC) at Brookhaven National Laboratory. The data on file at NNDC have not been corrected for the presence of ^{139}La resonances or for p-wave neutrons, and the assigned uncertainties are only those due to fission counting statistics.

III. RESOLVED RESONANCE ANALYSIS

The spin-separated fission cross sections of $(^{235}\mathrm{U}+n)$ are shown in Figs. 1–12 for the energy

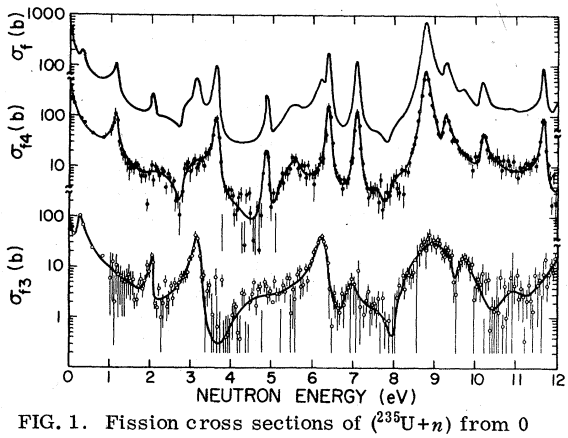

FIG. 1. Fission cross sections of $(^{235}\mathrm{U}+n)$ from 0 to 12 eV. The lower curve is the spin-3 fission cross section; the center curve is the spin-4 fission cross section; the top curve is the sum of the two lower curves, corresponding to the fission cross section measured with an unpolarized beam and target. Data below 1 eV are those of Schermer *et al.* (Ref. 14) normalized to the present measurement at the 1.14 eV resonance.

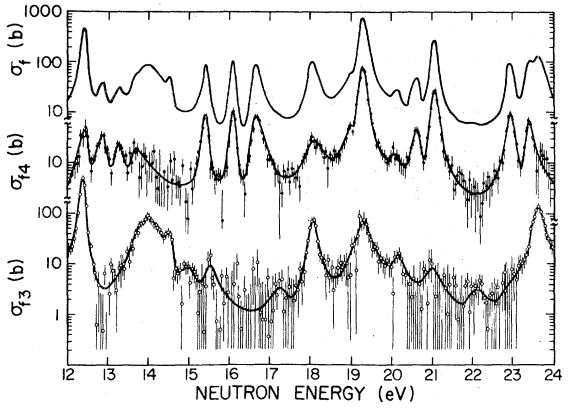

FIG. 2. Fission cross sections of (^{235}U+n) from 12 to 24 eV. The lower curve is the spin-3 fission cross section; the center curve is the spin-4 fission cross section; the top curve is the sum of the two lower curves, corresponding to the fission cross section measured with an unpolarized beam and target.

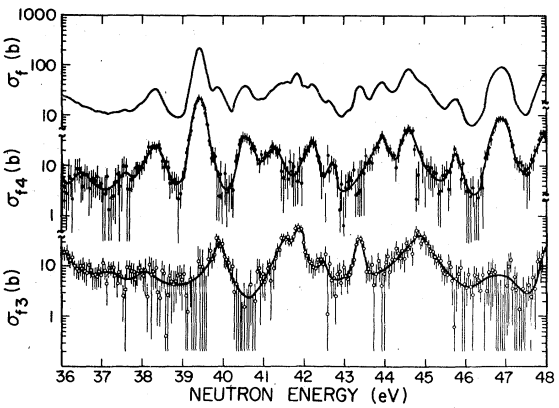

FIG. 4. Fission cross sections of (^{235}U+n) from 36 to 48 eV. The lower curve is the spin-3 fission cross section; the center curve is the spin-4 fission cross section; the top curve is the sum of the two lower curves, corresponding to the fission cross section measured with an unpolarized beam and target.

region below 300 eV. Data shown in Fig. 1 below 1 eV are those of Schermer *et al.*,[14] for which a data-reduction procedure similar to that described in the previous section for the region between 1.0 and 1.6 eV was carried out. The unknown nuclear polarization in the measurement of Schermer *et al.* was determined to be 4.8% by normalizing their point at 1.14 eV to the results of the present measurement. The top curve in Figs. 1–12 is the sum of σ_{f4} (the middle curve) and σ_{f3} (the lower curve) and corresponds to the fission cross section of (^{235}U+n) with an unpolarized beam and unpolarized target. The resolution in the present measurement is slightly poorer than that of Blons *et al.*,[15] but the statistical accuracy of the data shown as the top curve is much better than that of any fission data on (^{235}U+n) that has been previously reported.

It is apparent from Figs. 1–12 that there is little difficulty in assigning spins to the known, previously observed resonances; these results confirm all the spin assignments previously made by this technique for resonances in (^{235}U+n), i.e., those by Keyworth *et al.*,[6,7] by Schermer *et al.*,[14] and by Reddingius *et al.*[16] They show clearly the existence of several resonances that have not been previously reported. The only problem one has is in deciding which of the previously unobserved resonances are real and which are spurious.

Resonance parameters for (^{235}U+n) have been

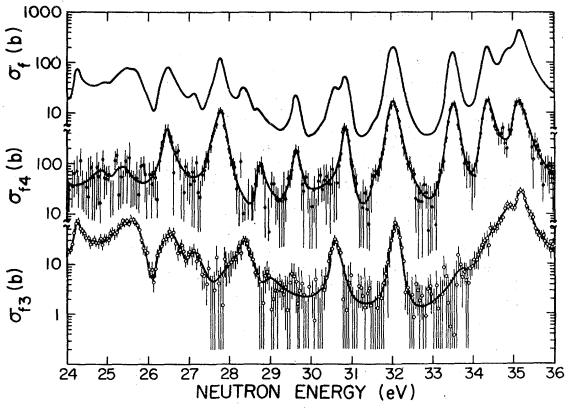

FIG. 3. Fission cross sections of (^{235}U+n) from 24 to 36 eV. The lower curve is the spin-3 fission cross section; the center curve is the spin-4 fission cross section; the top curve is the sum of the two lower curves, corresponding to the fission cross section measured with an unpolarized beam and target.

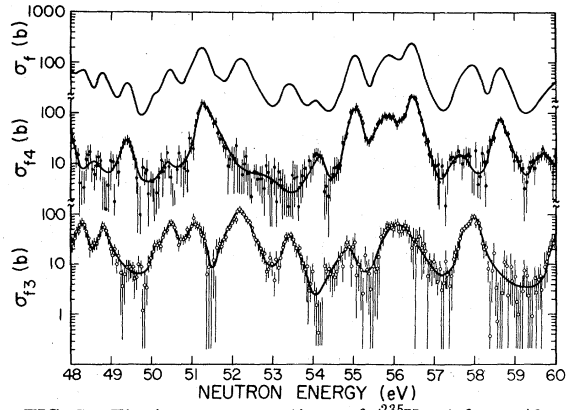

FIG. 5. Fission cross sections of (^{235}U+n) from 48 to 60 eV. The lower curve is the spin-3 fission cross section; the center curve is the spin-4 fission cross section; the top curve is the sum of the two lower curves, corresponding to the fission cross section measured with an unpolarized beam and target.

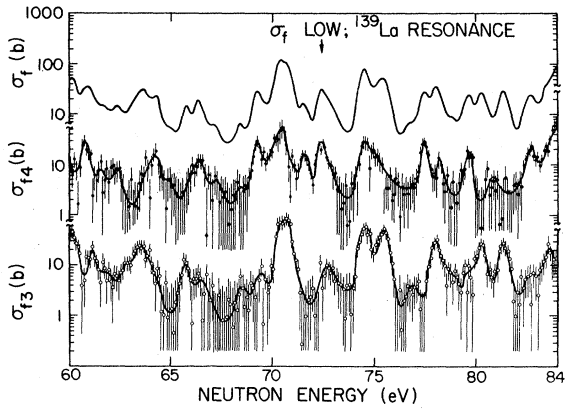

FIG. 6. Fission cross sections of (^{235}U+n) from 60 to 84 eV. The lower curve is the spin-3 fission cross section; the center curve is the spin-4 fission cross section; the top curve is the sum of the two lower curves, corresponding to the fission cross section measured with an unpolarized beam and target.

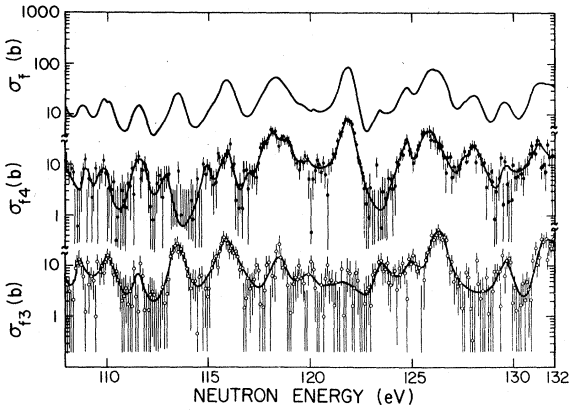

FIG. 8. Fission cross sections of (^{235}U+n) from 108 to 132 eV. The lower curve is the spin-3 fission cross section; the center curve is the spin-4 fission cross section; the top curve is the sum of the two lower curves, corresponding to the fission cross section measured with an unpolarized beam and target.

reported to 150 eV; from 150 to 300 eV only the resonance energies of prominent structure are known.[17] The analysis of the present data was done under the same constraints; Table III contains spin assignments and resonance energies to 300 eV, and fission areas to 150 eV. The resonances in Table III were divided into three categories: (1) resonances whose existence is considered definite, (2) resonances considered probable (shown in parentheses), and (3) resonances considered doubtful or unlikely (shown in brackets). Fission areas are preserved over broad energy bands containing several resonances for the first category, and the uncertainties reflect statistical uncertainties, wing correction uncertainties, and uncertainties arising from the possible existence of levels in categories 2 and 3, for which only upper limits of the fission areas are estimated.

Figure 13 shows a plot of the number of observed and probable resonances of each spin having $E_0 < E$ as a function of neutron energy. Examination of this figure suggests that below about 60 eV, a linear relationship holds, and that the fraction of missing levels is not energy dependent. Attempts to use the Dyson-Mehta Δ_3 statistic[18] or F statistic[19] to determine the number of missing levels were not satisfactory; the number of such levels is simply too large for these tests to be useful.

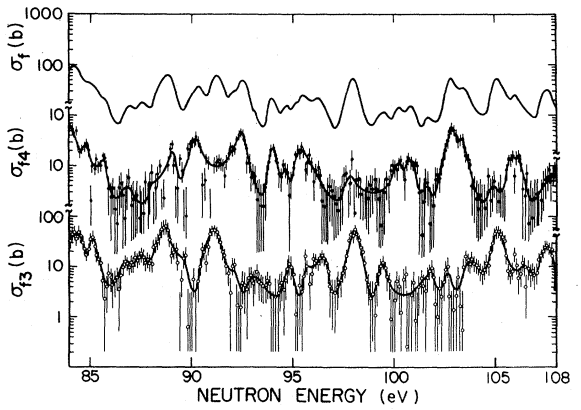

FIG. 7. Fission cross sections of (^{235}U+n) from 84 to 108 eV. The lower curve is the spin-3 fission cross section; the center curve is the spin-4 fission cross section; the top curve is the sum of the two lower curves, corresponding to the fission cross section measured with an unpolarized beam and target.

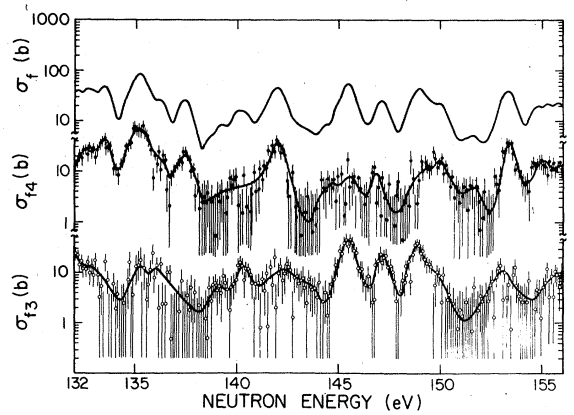

FIG. 9. Fission cross sections of (^{235}U+n) from 132 to 156 eV. The lower curve is the spin-3 fission cross section; the center curve is the spin-4 fission cross section; the top curve is the sum of the two lower curves, corresponding to the fission cross section measured with an unpolarized beam and target.

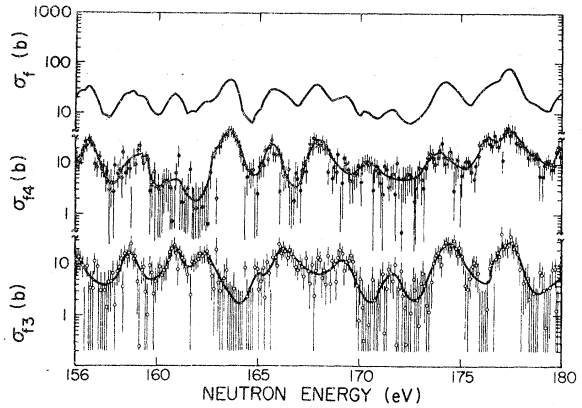

FIG. 10. Fission cross sections of (^{235}U+n) from 156 to 180 eV. The lower curve is the spin-3 fission cross section; the center curve is the spin-4 fission cross section; the top curve is the sum of the two lower curves, corresponding to the fission cross section measured with an unpolarized beam and target.

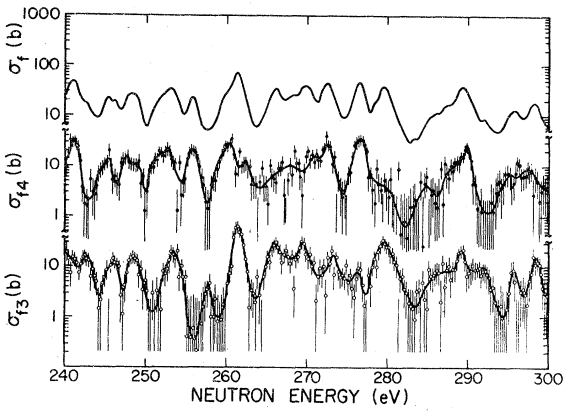

FIG. 12. Fission cross sections of (^{235}U+n) from 240 to 300 eV. The lower curve is the spin-3 fission cross section; the center curve is the spin-4 fission cross section; the top curve is the sum of the two lower curves, corresponding to the fission cross section measured with an unpolarized beam and target.

The next step in the analysis was the determination of the total width Γ for each resonance. This was done by calculating a series of Breit-Wigner line shapes and broadening them numerically with a function thought to be representative of the Doppler and resolution function. In this way, one constructs a series of curves that give the observed full width at half maximum as a function of the natural width for each resonance. It was found that this procedure is not very satisfactory unless the resonance in question is wide, strong, and fairly well isolated, because the statistical accuracy of the spin-separated data is low and the resolution function is not well known.

An alternative procedure, which was adopted, is to rely on previous measurements of the total, fission, and capture cross sections that have been carefully analyzed. In comparing the results of previous analyses, one finds that they share the same problem as that described above in deter-

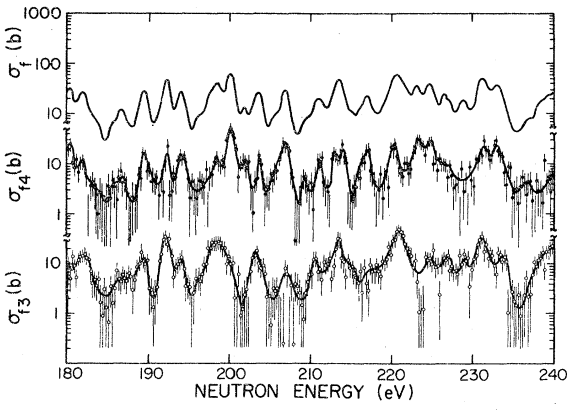

FIG. 11. Fission cross sections of (^{235}U+n) from 180 to 240 eV. The lower curve is the spin-3 fission cross section; the center curve is the spin-4 fission cross section; the top curve is the sum of the two lower curves, corresponding to the fission cross section measured with an unpolarized beam and target.

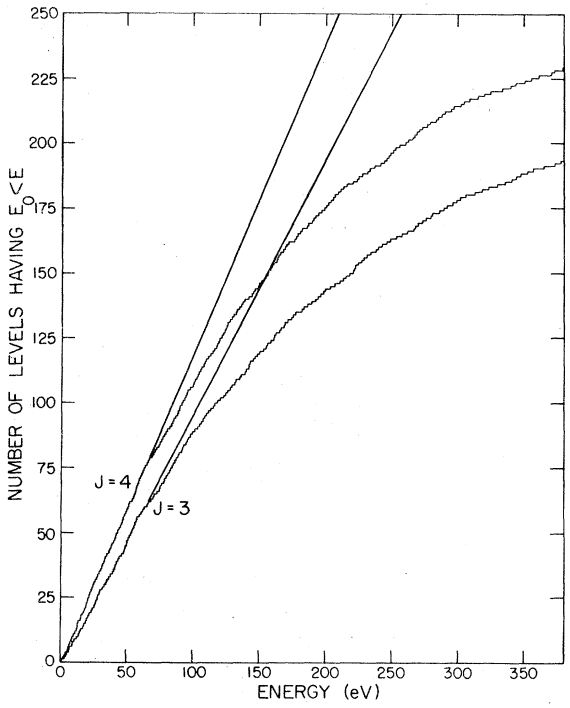

FIG. 13. The number of observed and probable resonances of each spin having $E_0 < E$ as a function of neutron energy below 380 eV. The top curve represents spin-4 resonances; the bottom curve spin-3 resonances. The fraction of missing resonances is independent of neutron energy below ~ 60 eV.

TABLE III. Spin assignments, resonance energies, and fission areas obtained from the present work. Resonances whose existence is considered probable are listed in parentheses; those considered doubtful in brackets.

J	E_0 (eV)	$\sigma_0\Gamma_f$ (beV)	J	E_0 (eV)	$\sigma_0\Gamma_f$ (beV)	J	E_0 (eV)	$\sigma_0\Gamma_f$ (beV)
4	1.14	···	4	[23.75]	≲1	3	(45.7)	≲0.9
3	2.03	1.3±0.3	3	24.25	12.8±3.2	4	45.73	3.5±0.9
4	2.8	~1	4	(24.3)	≲1	3	[46.2]	≲0.6
3	3.14	7.3±0.4	3	(24.4)	≲4	4	46.8	15.0±8.0
4	3.61	11.6±2.6	4	24.90	~1.6	3	46.9	4.0±2.0
3	4.2	~0.6	4	25.40	2.8±2.4	4	47.0	14.6±8.0
4	4.84	1.4±0.3	3	25.62	43.8±4.0	4	47.91	12.6±2.5
4	5.52	6.5±1.2	4	26.46	10.2±1.6	3	(47.95)	≲3
3	6.20	11.0±1.6	3	26.52	12.8±1.6	3	48.27	17.1±2.8
4	6.39	12.4±0.9	3	27.11	2.6±1.0	4	48.55	2.4±2.0
3	6.95	0.9±0.5	4	27.77	22.8±2.0	3	48.78	16.1±2.2
4	7.07	9.8±0.9	3	27.95	~0.5	(4)	(49.0)	···
4	7.55	~0.3	3	28.36	9.5±1.4	4	49.38	8.5±1.3
3	7.70	~0.5	4	28.76	1.3±0.3	3	50.08	1.7±0.9
4	[8.0]	≲0.5	3	29.0	1.3±0.5	4	50.36	~1.3
3	[8.2]	≲2	4	(29.15)	≲0.5	3	50.47	15.7±2.4
4	8.78	118 ±5	3	[29.55]	≲1.3	3	51.07	19.8±6.4
3	8.97	10.9±3.8	4	29.63	3.3±0.4	4	51.25	47.9±6.5
4	9.29	15.3±2.7	4	[30.3]	≲1.0	4	51.6	~6
3	9.71	4.2±0.6	3	30.59	6.1±0.9	3	[51.7]	≲3
4	10.18	6.4±2.9	4	30.83	9.2± 1.0	4	[52.05]	≲1
4	(10.8)	≲2	3	(31.3)	≲0.6	3	52.19	43.9±5.2
3	10.92	0.6±0.5	4	31.55	~0.5	4	52.9	~2
4	[11.3]	≲1	4	32.02	30.5± 3.5	4	[53.15]	≲2
4	11.64	12.1±2.9	3	32.08	10.2± 2.7	3	53.39	11.3±2.6
3	12.39	51.3±1.4	4	(32.52)	≲0.9	3	[53.65]	≲2.5
4	12.43	5.0±1.7	4	33.50	26.5± 2.2	4	54.11	4.6±1.2
4	12.85	6.2±0.5	3	33.65	~1.2	3	(54.3)	≲0.6
4	13.26	4.1±0.5	4	34.35	33.4± 3.5	3	54.88	8.0±4.3
4	13.68	6.3±2.0	3	34.4	13 ± 6	4	55.02	28.7±4.5
3	13.98	37.1±3.2	3	34.84	29.8± 9.4	4	55.78	42.0±5.0
4	(14.14)	≲2	4	35.11	44 ± 9	3	55.85	14.1±6.0
3	[14.2]	≲4	3	35.18	74.9±13	3	56.1	19.7±6.0
3	14.50	3.1±1.5	4	[35.9]	≲3	4	56.44	54.2±8.0
4	[14.6]	≲1.5	3	[36.1]	≲3	3	(57.02)	≲1
3	[14.95]	≲0.9	4	36.45	2.1± 0.8	4	57.61	3.7±3.1
4	15.39	12.6±0.9	3	(36.6)	≲1	3	57.70	12.7±4.0
3	15.51	~1	3	37.2	1.7± 0.7	3	57.97	17.1±4.0
4	16.08	11.0±0.7	4	37.57	1.4± 0.8	4	58.62	22.3±4.0
3	[16.2]	≲1	3	38.08	3.3± 1.6	3	(58.85)	≲0.7
4	16.67	16.7±0.9	4	38.29	9.9± 1.1	4	(59.12)	≲1
4	[17.0]	≲1	3	[38.89]	≲0.5	4	59.68	6.8±1.6
3	17.22	0.6±0.5	4	39.39	45.9± 1.2	3	60.16	16.5±2.5
3	18.05	13.7±1.8	3	39.88	8.8± 3.8	4	(60.25)	≲0.9
4	18.12	6.6±2.5	4	40.52	11.6± 1.2	4	60.75	9.9±1.8
4	18.96	~3	3	(40.88)	≲0.9	3	61.11	8.0±1.7
4	19.28	118 ±7	4	41.22	8.0± 1.7	4	61.62	~1
3	19.32	14.2±3.6	3	41.51	9.2± 1.6	3	61.96	2.1±0.8
4	20.08	1.2±1.0	3	41.81	13.9± 2.2	4	62.40	3.9±1.2
3	20.13	2.1±0.6	4	42.20	8.5± 2.1	3	62.85	2.5±1.0
4	20.61	6.5±1.0	3	42.46	2.2± 0.9	3	63.49	16.5±2.1
3	20.91	~0.8	4	42.68	1.5± 0.8	4	63.73	2.6±1.6
4	21.06	38.4±2.2	3	[42.85]	≲0.5	4	64.22	4.5±1.2
4	(21.5)	≲1	4	(43.2)	≲2	4	64.95	2.5±0.4
3	22.05	1.0±0.3	3	43.46	5.7± 1.6	3	65.73	3.2±0.7
4	22.92	14.9±1.0	4	43.93	12.6± 1.6	4	66.07	2.3±0.8
4	23.38	11.0±1.7	4	44.56	15.6± 2.8	4	66.38	3.3±0.8
3	23.61	32.8±3.0	3	44.86	25.5± 3.8	3	66.45	2.5±0.8

TABLE III. *(Continued)*.

J	E_0 (eV)	$\sigma_0\Gamma_f$ (beV)	J	E_0 (eV)	$\sigma_0\Gamma_f$ (beV)	J	E_0 (eV)	$\sigma_0\Gamma_f$ (beV)
4	(66.89)	≲1.2	3	96.4	8.8±1.5	4	133.5	19.7± 3.8
4	67.15	1.6± 0.3	4	97.8	~2	4	135.2	54.3± 7.5
4	(67.6)	≲0.5	3	98.05	23.3±2.9	3	135.3	~4.2
4	68.22	~0.5	4	(99.0)	≲1	3	136.0	6.8± 3.2
3	68.48	1.6± 0.4	3	99.4	3.7±0.9	4	136.4	3.8± 2.2
4	69.22	~0.5	4	100.25	7.8±2.1	4	137.4	14.2± 2.0
3	69.39	2.0± 1.4	3	(100.5)	1.8±1.2	3	(137.9)	≲0.9
4	70.10	7.7± 2.0	4	100.85	4.9±1.0	4	139.0	1.0± 0.7
3	70.30	16.6± 5.5	4	101.6	~0.7	3	139.1	2.7± 0.8
4	70.48	16.3± 6.3	3	101.8	3.0±0.8	4	(139.9)	2.9± 1.6
3	70.76	25.0± 5.5	3	102.65	~1.9	3	140.3	7.8± 1.7
4	71.55	5.6± 1.0	4	102.8	23.3±2.9	3	141.9	13.3± 1.4
4	72.4	13.4± 1.6	4	103.4	6.0±2.4	4	142.0	22.3± 3.8
3	72.69	4.4± 1.6	3	103.7	7.7±2.6	3	143.7	2.3± 0.9
3	74.51	20.6± 3.6	4	(104.8)	≲1	4	144.4	3.2± 1.2
4	74.55	9.3± 3.3	3	105.15	25.1±3.4	3	145.4	26.8± 4.1
4	75.02	7.3± 3.6	4	105.7	4.7±2.4	4	145.6	5.1± 4.3
3	75.42	20.2± 2.9	4	106.1	3.1±2.4	4	146.8	3.0± 2.3
4	76.2	~1.4	3	106.4	3.5±1.5	3	147.2	11.2± 2.3
3	76.9	~1	3	107.55	12.4±2.2	4	(148.6)	≲2
4	77.46	9.9± 1.6	4	(107.6)	≲1.8	3	148.9	19.4± 3.7
3	78.0	12.1± 2.2	4	108.1	3.6±2.2	4	149.9	5.9± 3.8
4	78.17	3.9± 1.9	3	108.6	4.9±1.2	3	150.0	2.7± 2.4
3	78.8	2.0± 1.6	4	109.0	2.2±1.0	4	(151.2)	
3	79.53	2.4± 1.2	4	109.85	3.4±1.5	4	151.6	
4	79.66	6.5± 1.5	3	110.1	8.5±1.5	3	152.9	
3	80.28	9.2± 1.5	3	111.5	1.7±1.1	4	153.4	
4	80.8	3.3± 2.0	4	111.6	6.3±1.1	4	154.8	
3	81.3	10.6± 1.5	4	112.8	2.4±1.6	3	155.4	
3	82.7	1.8± 1.1	3	113.4	14.0±1.7	4	155.8	
4	82.75	8.5± 1.5	4	114.9	1.9±1.2	3	156.1	
3	83.6	7.2± 3.2	3	115.8	23.5±3.6	4	156.7	
4	84.0	42.3± 6.3	4	115.9	9.7±3.8	4	(157.5)	
3	84.3	23.1± 6.1	4	116.8	1.3±0.9	4	(158.2)	
4	84.8	4.5± 3.3	3	(117.2)	≲1	3	158.6	
3	85.1	10.2± 1.5	4	(117.7)	≲6	4	159.2	
4	85.7	3.1± 1.3	4	118.1	25.5±4.2	4	160.8	
3	(85.9)	···	3	118.45	8.2±5.2	3	160.9	
3	86.75	3.2± 1.0	4	118.9	14.5±3.0	4	(161.7)	
4	86.85	1.5± 1.3	3	(119.4)	~1.2	3	162.3	
3	87.5	8.5± 1.4	4	(119.8)	~3.9	4	(162.8)	
4	88.2	~2	3	120.0	~1.3	4	163.6	
3	88.7	33.0± 4.2	4	(120.5)	≲2	3	164.9	
4	89.05	7.0± 3.4	3	121.6	~3.8	4	165.7	
3	89.7	~1.3	4	121.8	44.5± 5.0	3	166.3	
4	90.0	~8	3	123.5	5.7± 1.3	4	168.0	
4	90.4	9.3± 8.0	4	124.7	11.4± 2.7	3	169.3	
3	91.1	28.0± 4.5	3	125.0	6.2± 3.2	4	170.4	
4	(91.4)	≲1.5	4	125.7	17.0±10.0	3	171.6	
4	92.0	~4	4	126.0	23.3±10.0	4	(173.3)	
3	92.15	~0.8	3	126.3	27.8± 6.8	4	174.0	
4	92.45	21.1± 3.6	4	127.5	2.1± 1.2	3	174.4	
3	93.15	4.3± 2.0	3	(128.0)	≲1.5	4	(175.3)	
4	94.0	7.5± 1.2	4	128.1	13.8± 2.1	3	(175.7)	
4	94.65	1.5± 0.9	4	129.5	2.9± 1.6	4	176.3	
3	94.85	3.9± 1.5	3	129.6	6.3± 1.6	3	177.3	
4	(95.2)	≲1	4	131.2	16.4± 4.1	4	177.4	
4	95.5	14.0± 3.1	3	131.6	24.5± 5.2	4	178.7	
3	95.7	1.4± 1.0	4	132.6	18.1± 4.7	4	(179.3)	
4	(95.9)	≲2	3	133.0	5.4± 5.1	4	180.0	

TABLE III. *(Continued)*.

J	E_0 (eV)	J	E_0 (eV)	J	E_0 (eV)
3	180.5	3	213.4	3	253.9
4	181.7	4	213.8	4	255.7
3	182.2	3	215.2	3	257.8
4	183.4	4	216.0	4	259.2
3	(183.8)	4	217.0	4	260.4
4	185.6	3	217.5	3	261.4
3	186.1	4	220.3	4	262.2
4	186.6	3	220.8	4	264.4
3	187.5	4	223.3	3	266.0
3	189.2	3	224.6	4	267.7
4	189.5	4	224.7	3	269.6
3	(189.8)	3	226.6	4	270.7
4	191.1	4	227.0	4	272.5
3	192.2	3	228.8	3	273.1
4	192.4	3	231.1	4	276.6
3	194.0	4	231.4	3	276.8
4	194.1	4	232.9	3	278.5
3	196.0	3	233.6	3	279.4
3	197.8	4	236.5	4	280.5
4	198.4	3	238.0	4	284.5
4	200.2	3	239.8	3	285.5
4	201.8	4	241.0	4	287.0
3	203.2	3	242.6	3	289.1
4	203.6	4	244.0	4	289.8
4	205.2	4	245.3	3	292.1
4	206.7	3	245.9	4	294.5
3	207.0	4	247.5	3	295.6
4	209.5	3	247.8	4	296.1
3	210.6	4	249.0	4	297.5
4	211.2	4	251.5	3	298.4
4	212.9	4	252.7	3	300.6

mining the total widths; i.e., the total widths determined by shape analysis are so strongly dependent on what is assumed for the resolution function that no meaningful comparison can be made. There are but two quantities that seem to be reasonably well represented by such analyses, the total area $\sigma_0\Gamma$ and the fission area $\sigma_0\Gamma_f$. The procedure used to obtain resonance parameters was to calculate total and fission areas from previous results of fitting total and partial cross sections.[15,20-34] We then selected results that were in reasonable agreement from Refs. 15, 20, 27–29, 31, 32, and 34, averaged them, and obtained the standard deviation. If the resonance in question is isolated, the fission areas generally agree, within the errors, with the corresponding entry in Table III. If the resonance in question consists of a mixed doublet of different spin, which is often the case, we used our estimated total width for the wider of the two, calculated $\sigma_0\Gamma$ from $\sigma_0\Gamma_f$ and our estimate of the total width, using an assumed value of 35 meV for Γ_γ, and obtained $\sigma_0\Gamma$ for the narrower of the two by subtraction. If the resonance in question consists of more than two components, then we proceeded by stripping the one with the largest apparent width, then the next largest, etc., with a corresponding increase in the uncertainty. It should be emphasized that this procedure depends on an estimate of the total width for the wider of two previously unresolved levels. Below 60 eV, the procedure is reasonably satisfactory, but at the higher energies in the range of 60–100 eV, the estimate of the total width becomes much less reliable. At energies above 100 eV, where the resolution width approaches 0.5 eV, this resonance analysis procedure could not be used.

The recommended parameters are listed in Table IV. They are not multilevel parameters and are not expected to describe the resonance asymmetries. The objective is to provide a more nearly complete set of parameters that preserve the spin-dependent fission strength reflected in the present work, that are consistent with capture and

TABLE IV. Recommended resonance parameters for ($^{235}U + n$) below 100 eV. The assumption is made that $\Gamma_\gamma = 35 \pm 2$ meV for both spin states.

J	E_0 (eV)	$2g\Gamma_n^0$ (meV)	Γ_f (meV)	$\sigma_0\Gamma$ (meV)	$\sigma_0\Gamma_f$ (meV)
3	0.285 ± 0.007	0.0059 ± 0.0011	86 ± 17	14.5 ± 2.6	10.3 ± 1.9
4	1.144 ± 0.015	0.0129 ± 0.0014	107 ± 11	15.8 ± 1.7	11.9 ± 1.1
3	2.033 ± 0.003	0.0057 ± 0.0004	10.7 ± 1.2	5.22 ± 0.36	1.22 ± 0.12
4	2.762 ± 0.013	0.00078 ± 0.00028	74 ± 28	0.62 ± 0.22	0.42 ± 0.16
3	3.150 ± 0.007	0.0122 ± 0.0008	103 ± 11	9.0 ± 0.6	6.8 ± 0.6
4	3.613 ± 0.006	0.0250 ± 0.0012	52.8 ± 4.7	17.3 ± 0.8	10.4 ± 0.7
3	4.2 ± 0.2	~0.0011	~200 [a]	~0.7	~0.6
4	4.845 ± 0.004	0.0276 ± 0.0007	3.9 ± 0.6	16.5 ± 0.4	1.66 ± 0.22
4	5.50 ± 0.08	0.0134 ± 0.0009	400 ± 60	7.5 ± 0.5	6.9 ± 0.9
3	6.214 ± 0.023	0.0275 ± 0.0057	132 ± 27	12.4 ± 3.0	9.8 ± 1.9
4	6.382 ± 0.015	0.1077 ± 0.0060	11.0 ± 2.1	56.0 ± 3.1	13.3 ± 2.4
3	6.95 ± 0.03	0.0020 ± 0.0012	330 ± 30 [a]	1.0 ± 0.6	0.9 ± 0.5
4	7.077 ± 0.003	0.0458 ± 0.0016	27.9 ± 2.7	22.6 ± 0.8	10.0 ± 0.8
4	7.55 ± 0.01	~0.0013	~35 [a]	~0.6	~0.3
3	7.70 ± 0.05	~0.0013	~200 [a]	~0.6	~0.5
4	8.766 ± 0.019	0.370 ± 0.021	98 ± 9	164 ± 9	120 ± 9
3	8.97 ± 0.03	0.026 ± 0.009	650 ± 50 [a]	11.5 ± 4.0	10.9 ± 3.8
4	9.279 ± 0.010	0.051 ± 0.015	83 ± 30	21.9 ± 6.4	15.4 ± 5.5
3	9.76 ± 0.04	0.0107 ± 0.0024	320 ± 30 [a]	4.6 ± 1.0	4.2 ± 0.6
4	10.177 ± 0.021	0.0202 ± 0.0039	62 ± 13	8.3 ± 1.6	5.3 ± 1.1
3	10.9 ± 0.1	~0.0018	~210 [a]	~0.7	~0.6
4	11.669 ± 0.012	0.174 ± 0.010	5.8 ± 1.1	67.1 ± 3.9	9.4 ± 1.7
3	12.396 ± 0.004	0.366 ± 0.016	22.7 ± 2.2	136.5 ± 6.0	52.4 ± 4.2
4	12.43 ± 0.03	0.0172 ± 0.0054	125 ± 40 [a]	6.4 ± 2.0	5.0 ± 1.7
4	12.862 ± 0.015	0.0213 ± 0.0016	109 ± 18	7.8 ± 0.6	5.9 ± 0.9
4	13.270 ± 0.026	0.0147 ± 0.0039	134 ± 48	5.3 ± 1.4	4.2 ± 1.5
4	13.696 ± 0.022	0.016 ± 0.010	57 ± 30	5.5 ± 3.6	3.4 ± 1.7
3	13.996 ± 0.013	0.128 ± 0.019	560 ± 80	45.0 ± 6.7	42.3 ± 5.4
3	14.552 ± 0.023	0.0279 ± 0.0035	18.4 ± 4.6	9.6 ± 1.2	3.3 ± 0.8
4	15.408 ± 0.007	0.0616 ± 0.0018	42.8 ± 3.6	20.6 ± 0.6	11.3 ± 0.7
3	15.51 ± 0.01	~0.0036	~175 [a]	~1.2	~1
4	16.090 ± 0.007	0.0940 ± 0.0021	20.5 ± 2.5	30.8 ± 0.7	11.3 ± 1.2
4	16.664 ± 0.016	0.0699 ± 0.0025	97 ± 8	22.5 ± 0.8	16.5 ± 1.1
3	17.22 ± 0.02	~0.0025	~105 [a]	~0.8	~0.6
3	18.05 ± 0.02	0.063 ± 0.010	89 ± 18	19.4 ± 3.2	13.9 ± 2.7
4	18.12 ± 0.03	0.024 ± 0.010	260 ± 70 [a]	7.4 ± 3.0	6.6 ± 2.5
4	18.972 ± 0.016	0.0235 ± 0.0046	32 ± 14	7.1 ± 1.4	3.4 ± 1.5
4	19.297 ± 0.015	0.667 ± 0.029	53.2 ± 4.9	200. ± 9.	117. ± 9
3	19.32 ± 0.03	0.054 ± 0.013	220 ± 70 [a]	16.3 ± 4.0	14.2 ± 3.6
4	20.08 ± 0.03	0.010 ± 0.006	25 ± 20	2.9 ± 1.6	1.2 ± 1.0
3	20.17 ± 0.04	0.009 ± 0.004	125 ± 35 [a]	2.7 ± 1.2	2.1 ± 0.6
4	20.63 ± 0.03	0.0401 ± 0.0021	41.7 ± 4.1	11.6 ± 0.6	6.3 ± 0.5
3	20.91 ± 0.04	~0.0031	~280 [a]	~0.9	~0.8
4	21.068 ± 0.014	0.334 ± 0.024	24.0 ± 2.3	95.5 ± 6.9	38.0 ± 3.0
3	22.05 ± 0.03	~0.0036	~260 [a]	~1.0	~0.9
4	22.934 ± 0.025	0.0962 ± 0.0047	44.5 ± 4.4	26.4 ± 1.3	14.7 ± 1.2
4	23.411 ± 0.009	0.164 ± 0.012	11.8 ± 3.1	44.4 ± 3.4	11.0 ± 2.8
3	23.612 ± 0.015	0.163 ± 0.016	126. ± 18	44.1 ± 4.3	34.3 ± 4.4
3	24.23 ± 0.02	0.069 ± 0.006	30.7 ± 4.3	18.3 ± 1.5	8.5 ± 1.1
4	24.90 ± 0.04	~0.0072	~160 [a]	~1.9	~1.6
4	25.40 ± 0.04	~0.0127	~160 [a]	~3.3	~2.8
3	25.60 ± 0.02	0.218 ± 0.023	550 ± 60	56.6 ± 6.0	53.1 ± 5.7
4	26.46 ± 0.02	0.064 ± 0.011	58 ± 10	16.4 ± 2.8	10.2 ± 1.6
3	26.52 ± 0.04	0.054 ± 0.008	440 ± 60 [a]	13.8 ± 2.0	12.8 ± 1.6
3	27.16 ± 0.03	0.0147 ± 0.0048	65 ± 25	3.7 ± 1.2	2.4 ± 0.9
4	27.79 ± 0.03	0.124 ± 0.024	91 ± 7	30.9 ± 5.9	22.2 ± 1.3
3	28.00 ± 0.05	0.0077 ± 0.0036	100 ± 60	1.8 ± 0.9	1.4 ± 0.8
3	28.36 ± 0.02	0.0365 ± 0.0041	109 ± 16	9.0 ± 1.0	6.8 ± 0.9
4	28.73 ± 0.03	0.0078 ± 0.0057	40 ± 25	1.9 ± 1.4	1.0 ± 0.7

TABLE IV. *(Continued)*

J	E_0 (eV)	$2g\Gamma_n^0$ (meV)	Γ_f (meV)	$\sigma_0\Gamma$ (meV)	$\sigma_0\Gamma_f$ (meV)
3	29.00 ±0.05	~0.0057	~260 [a]	~1.4	1.3±0.5
4	29.656±0.020	0.0319±0.0021	23.7± 3.3	7.7± 0.5	3.1±0.4
3	30.593±0.015	0.038 ±0.007	87 ± 12	9.0± 1.6	6.4±0.8
4	30.869±0.015	0.097 ±0.006	19.8± 4.3	22.9± 1.5	8.2±1.7
4	31.55 ±0.02	~0.0026	~160 [a]	~0.6	~0.5
4	32.02 ±0.02	0.191 ±0.040	85. ± 30 [a]	44.3± 9.4	31.4±3.6
3	32.08 ±0.03	0.138 ±0.047	16.8± 6.5	32 ±11	10.2±2.7
4	33.518±0.013	0.309 ±0.013	27.0± 2.6	70.2± 3.0	29.8±2.3
3	33.65 ±0.03	~0.0079	~70 [a]	~1.8	~1.2
4	34.373±0.017	0.340 ±0.031	28.6± 4.2	76.3± 7.0	33.4±4.5
3	34.4 ±0.1	0.039 ±0.027	730 ±470	8.7± 6.0	8.3±5.3
3	34.858±0.017	0.192 ±0.032	76 ± 14	42.8± 7.0	28.9±5.0
4	35.11 ±0.03	0.239 ±0.050	170 ± 40 [a]	53 ±11	44 ±9
3	35.18 ±0.03	0.578 ±0.068	100 ± 15	128 ±15	92 ±13
4	36.45 ±0.03	0.012 ±0.009	125 ± 80 [a]	2.7± 2.0	2.1±0.8
3	37.20 ±0.05	0.0093±0.0046	200 ± 80 [a]	2.0± 1.0	1.7±0.7
4	37.57 ±0.03	0.0079±0.0047	160 ± 80 [a]	1.7± 1.0	1.4±0.8
3	38.08 ±0.03	0.018 ±0.009	230 ±100 [a]	3.8± 2.0	3.3±1.6
4	38.36 ±0.04	0.054 ±0.007	218 ± 27 [a]	11.5± 1.5	9.9±1.1
4	39.410±0.012	0.393 ±0.014	56.3± 4.2	82.2± 2.9	49.5±2.5
3	39.93 ±0.04	0.052 ±0.010	164 ± 71	10.7± 2.0	8.8±3.8
4	40.51 ±0.03	0.0673±0.0058	161 ± 17	13.9± 1.2	11.4±1.0
4	41.33 ±0.04	0.049 ±0.010	140 ± 50 [a]	10.0± 2.0	8.0±1.7
3	41.60 ±0.04	0.062 ±0.015	190 ± 70	12.7± 3.1	10.7±4.0
3	41.873±0.013	0.202 ±0.014	15.3± 1.6	40.9± 2.9	12.1±1.1
4	42.22 ±0.04	0.063 ±0.010	66.7± 6.8	12.7± 2.0	8.3±0.7
3	42.46 ±0.04	0.0134±0.0060	155. ± 70 [a]	2.7± 1.1	2.2±0.9
4	42.70 ±0.02	0.0418±0.0035	7.7± 4.1	8.4± 0.7	1.5±0.8
3	43.40 ±0.02	0.100 ±0.009	18.4± 3.4	20.0± 1.8	6.8±1.2
4	43.97 ±0.03	0.084 ±0.015	161 ± 37	16.6± 3.0	13.6±3.0
4	44.60 ±0.04	0.107 ±0.028	99 ± 34	21.1± 5.5	15.5±5.2
3	44.86 ±0.04	0.137 ±0.020	660 ±100	26.9± 4.0	25.5±3.8
4	45.82 ±0.04	0.0258±0.0031	100 ± 10	5.0± 0.6	3.7±0.3
4	46.80 ±0.04	0.101 ±0.025	103 ±29	19.4± 4.8	14.4±4.0
3	46.9 ±0.1	0.022 ±0.010	460 ±180 [a]	4.3± 2.0	4.0±2.0
4	47.02 ±0.05	0.122 ±0.029	68 ± 16	23.3± 5.5	15.3±3.6
4	47.97 ±0.02	0.128 ±0.017	38.8± 8.0	24.2± 3.3	12.6±2.5
3	48.31 ±0.02	0.142 ±0.031	115 ± 20	26.8± 5.9	20.4±3.3
4	48.55 ±0.05	~0.0154	~160 [a]	~2.9	2.4±2.0
3	48.77 ±0.03	0.116 ±0.014	50.5± 9.9	21.9± 2.7	12.8±2.4
4	49.45 ±0.04	0.142 ±0.017	16.9± 2.7	26.6± 3.1	8.5±1.3
3	50.12 ±0.04	0.044 ±0.008	34 ± 12	8.2± 1.5	4.0±1.4
4	50.40 ±0.04	~0.014	~35 [a]	~2.6	~1.3
3	50.51 ±0.04	0.121 ±0.016	49.4± 8.1	22.3± 3.0	12.9±2.0
3	51.11±0.04	0.122 ±0.038	260 ±80 [a]	22.4± 7.0	19.8±6.4
4	51.29±0.04	0.360 ±0.046	67 ±12	66.0± 8.5	42.5±7.3
4	51.63±0.03	0.064 ±0.015	60 ±30	11.7± 2.7	7.4±3.7
3	52.26±0.03	0.362 ±0.023	420 ±40	65.8± 4.1	60.3±4.3
4	52.9 ±0.2	~0.014	~120 [a]	~2.6	~2
3	53.46±0.05	0.084 ±0.009	96 ±14	15.1± 1.6	11.0±1.5
4	54.13±0.06	0.033 ±0.009	125 ±33	5.9± 1.6	4.6±1.2
3	54.92±0.04	0.052 ±0.026	220 ±100 [a]	9.3± 4.6	8.0±4.3
4	55.07±0.04	0.361 ±0.038	35.2± 5.7	63.9± 6.8	31.0±4.7
4	55.82±0.04	0.325 ±0.040	285 ± 35	57.2± 7.0	50.6±6.0
3	55.9 ±0.3	0.118 ±0.061	250 ±130	20.7±10.7	18.1±9.4
3	56.2 ±0.3	0.131 ±0.039	360 ±100 [a]	22.9± 6.8	20.9±6.4
4	56.50±0.06	0.490 ±0.058	53 ± 10	85.7±10.2	49.6±9.3
4	57.66±0.06	~0.024	~260 [a]	~4.2	3.7±3.1
3	57.81±0.06	0.126 ±0.025	110 ± 32	21.8± 4.3	16.4±4.7
3	58.10±0.06	0.178 ±0.013	38.5± 4.5	30.6± 2.2	15.7±1.6

TABLE IV. *(Continued)*

J	E_0 (eV)	$2g\Gamma_n^0$ (meV)	Γ_f (meV)	$\sigma_0\Gamma$ (meV)	$\sigma_0\Gamma_f$ (meV)
4	58.67±0.05	0.166 ±0.012	118 ± 9	28.5± 2.1	21.8±1.0
4	59.73±0.06	0.053 ±0.012	180 ± 80[a]	9.0± 2.0	7.5±1.8
3	60.20±0.05	0.137 ±0.014	143 ± 26	23.2± 2.3	18.5±3.2
4	60.82±0.06	0.075 ±0.018	130 ± 25	12.6± 3.1	9.9±1.8
3	61.13±0.06	0.069 ±0.018	79 ± 17	11.6± 3.0	8.0±1.7
4	61.62±0.06	~0.0072	~175[a]	~1.2	~1
3	61.96±0.06	~0.0138	~400[a]	~2.3	2.1±0.8
4	62.4 ±0.1	0.025 ±0.012	460 ±140[a]	4.2± 2.0	3.9±1.2
3	62.92±0.07	0.018 ±0.009	220 ±100[a]	2.9± 1.5	2.5±1.0
3	63.56±0.08	0.106 ±0.018	600 ±130[a]	17.5± 3.0	16.5±2.1
4	63.80±0.07	0.020 ±0.012	160 ±100[a]	3.2± 2.0	2.6±1.6
4	64.30±0.07	0.150 ±0.006	6.8± 1.1	24.5± 1.0	3.9±0.6
4	65.01±0.07	0.017 ±0.006	360 ±100[a]	2.7± 1.0	2.5±0.4
3	65.80±0.07	0.0457±0.0056	27.0± 6.1	7.4± 0.9	3.2±0.5
4	66.14±0.08	0.019 ±0.009	101 ± 40	3.1± 1.5	2.3±0.8
4	66.45±0.07	0.029 ±0.012	83 ± 21	4.7± 2.1	3.3±0.8
3	66.52±0.07	0.017 ±0.006	460 ±100[a]	2.7± 1.1	2.5±0.8
4	67.26±0.09	0.0156±0.0025	62 ± 12	2.5± 0.4	1.6±0.3
4	68.3 ±0.1	~0.0063	~35	~1.0	~0.5
3	68.55±0.09	0.0120±0.0050	160 ± 80[a]	1.9± 0.8	1.6±0.4
4	69.31±0.08	0.077 ±0.013	145 ± 16	12.2± 2.0	9.8±0.9
3	69.45±0.08	~0.005	~115[a]	~2.6	2.0±1.4
4	70.17±0.09	0.138 ±0.080	22.3± 10.2	21.7±12.4	8.3±2.2
3	70.37±0.09	0.132 ±0.041	220 ± 80[a]	20.7± 6.5	17.9±5.9
4	70.55±0.09	0.141 ±0.047	140 ± 80[a]	22.0± 7.4	17.6±6.8
3	70.83±0.09	0.196 ±0.048	260 ±120[a]	30.6± 7.5	27.0±5.9
4	71.59±0.09	0.055 ±0.013	68 ± 13	8.5± 1.8	5.6±1.0
4	72.41±0.06	0.334 ±0.028	79.8± 6.2	51.6± 4.3	35.1±2.0[b]
3	72.9 ±0.1	0.038 ±0.006	214 ± 35	5.9± 0.9	5.1±0.8[b]
3	74.57±0.08	0.161 ±0.028	260 ±100[a]	24.5± 4.2	21.6±3.8
4	74.62±0.08	0.179 ±0.037	20 ± 7	27.2± 5.6	9.8±3.5
3	75.5 ±0.1	0.154 ±0.032	370 ±120[a]	23.3± 4.8	21.2±3.1
4	75.2 ±0.1	0.081 ±0.040	60 ± 30	12.2± 6.1	7.7±3.8
4	76.3 ±0.1	~0.011	~260[a]	~1.6	~1.4
3	76.79±0.09	0.0122±0.0028	82 ± 32	1.8± 0.4	1.3±0.5
4	77.53±0.07	0.107 ±0.017	59 ± 10	15.9± 2.6	9.9±1.6
3	78.1 ±0.1	0.090 ±0.018	320 ±100[a]	13.4± 2.6	12.1±2.2
4	78.25±0.10	0.040 ±0.035	70 ± 50	5.9± 5.2	3.9±1.9
3	78.8 ±0.1	0.0212±0.004	130 ± 8	3.1± 0.7	2.5±0.5
3	79.6 ±0.1	0.039 ±0.035	25 ± 15	5.8± 5.1	2.4±1.2
4	79.7 ±0.1	0.048 ±0.034	440 ±100[a]	7.0± 5.0	6.5±1.5
3	80.4 ±0.1	0.084 ±0.010	140 ± 15	12.3± 1.4	9.8±0.9
4	80.9 ±0.1	0.025 ±0.020	360 ±240[a]	3.6± 3.0	3.3±2.0
3	81.45±0.1	0.101 ±0.007	87 ± 8	14.7± 1.0	10.4±0.7
3	82.7 ±0.1	~0.015	~200[a]	~2.1	1.8±1.1
4	82.75±0.1	0.210 ±0.022	14.5± 2.7	30.3± 3.2	8.6±1.5
3	83.6 ±0.1	0.112 ±0.028	29 ± 13	16.1± 4.0	7.2±3.2
4	84.1 ±0.1	0.328 ±0.070	320 ±100[a]	47 ±10	42.3±6.3
3	84.4 ±0.1	0.206 ±0.070	135 ± 40	29.4±10	23.1±6.1
4	84.8 ±0.1	~0.036	~260[a]	~5.1	4.5±3.3
3	85.1 ±0.1	0.085 ±0.028	190 ± 50	12.1± 4.0	10.2±1.5
4	85.7 ±0.1	0.027 ±0.020	160 ± 80	3.8± 2.9	3.1±1.3
3	86.8 ±0.1	0.027 ±0.021	~200[a]	3.8± 3.0	3.2±1.0
4	86.9 ±0.1	0.026 ±0.014	24 ± 20	3.7± 2.9	1.5±1.3
3	87.5 ±0.1	0.077 ±0.020	130 ± 30	10.8± 2.8	8.5±1.4
4	88.2 ±0.1	~0.021	~80[a]	~2.9	~2
3	88.7 ±0.1	0.266 ±0.072	300 ± 40	37.1±10	33.0±4.2
4	89.1 ±0.1	0.067 ±0.048	110 ± 60	9.3± 6.7	6.9±4.8
3	89.7 ±0.1	~0.011	~200[a]	~1.5	~1.3

TABLE IV. *(Continued)*

J	E_0 (eV)	$2g\Gamma_n^0$ (meV)	Γ_f (meV)	$\sigma_0\Gamma$ (meV)	$\sigma_0\Gamma_f$ (meV)
4	89.9 ±0.1	0.070 ±0.036	90 ± 50	9.7± 5.0	7.0±4.0
4	90.4 ±0.1	0.494 ±0.043	7.9± 2.8	68.3± 6.1	11.5±3.8
3	91.3 ±0.1	0.250 ±0.048	165 ± 30	34.4± 6.6	28.0±4.5
4	92.1 ±0.1	0.075 ±0.015	45 ± 16	10.2± 2.1	5.7±1.8
3	92.2 ±0.1	~0.0073	~200 [a]	~1	~0.8
4	92.6 ±0.1	0.270 ±0.033	30.7± 4.0	36.8± 4.5	16.6±4.5
3	93.2 ±0.1	~0.038	~200 [a]	~5.1	4.3±2.0
4	94.1 ±0.1	0.412 ±0.030	6.0± 1.0	55.8± 4.0	7.5±1.2
4	94.7 ±0.1	0.019 ±0.015	53 ± 32	2.5± 2.1	1.5±0.9
3	94.9 ±0.1	0.036 ±0.015	140 ± 50	4.9± 2.1	3.9±1.5
4	95.2 ±0.2	~0.010	~70 [a]	~1.5	~1
4	95.6 ±0.1	0.160 ±0.027	68 ± 16	21.5± 3.6	14.0±3.1
3	95.7 ±0.1	~0.013	~180 [a]	~1.7	1.4±1.0
4	96.1 ±0.1	0.042 ±0.013	41 ± 14	5.6± 1.8	3.0±1.0
3	96.5 ±0.1	0.085 ±0.019	122 ± 26	11.4± 2.5	8.8±1.8
4	97.9 ±0.1	~0.023	~70 [a]	~3	~2
3	98.1 ±0.1	0.253 ±0.034	86 ± 12	33.6± 4.5	23.3±2.9
3	99.5 ±0.1	0.045 ±0.014	60 ± 15	5.9± 1.8	3.7±0.9

[a] Fission widths for these resonances were obtained from estimates of the total widths observed in the present work, as described in the text. The corresponding entries for $\sigma_0\Gamma$ were calculated from these estimates by using $\sigma_0\Gamma_f$ and Γ_f under the assumption that $\Gamma_\gamma = 35$ meV.

[b] The presence of the large lanthanum resonance in this region precludes using the present data in obtaining resonance parameters, except for the spin assignment.

total cross section data, and that can be used to obtain average parameters for the statistical treatment of the unresolved resonance region.

IV. AVERAGE PARAMETERS IN THE RESOLVED RESONANCE REGION

A. Level spacings and reduced neutron widths

The tests based on calculation of the Dyson-Mehta Δ_3 statistic[18] were found to be unsatisfactory, because changing the criterion for levels that are included in the basis set can lead to completely different solutions for the average spacing. As an alternate approach, we devised an independent missing-level estimator, which is based on the properties of the reduced neutron width distribution. In particular, one uses the moments of the reduced neutron width distribution to estimate the number of missing levels. The following two assumptions are made: (1) the neutron width distribution is Porter-Thomas, and (2) the larger widths are accurately known. If it is assumed that the larger widths are known above $\langle\Gamma_n^0\rangle/4$, then it can easily be shown that the Porter-Thomas distribution has the following properties:

$$\int_{1/4}^{\infty} f(x)dx = 0.617\,, \tag{8a}$$

$$\int_{1/4}^{\infty} \sqrt{\Gamma_n^0} f(x)dx = 0.704\langle\Gamma_n^0\rangle^{1/2}\,, \tag{8b}$$

and

$$\int_{1/4}^{\infty} \Gamma_n^0 f(x)dx = 0.969\langle\Gamma_n^0\rangle\,, \tag{8c}$$

where $x = \Gamma_n^0/\langle\Gamma_n^0\rangle$, and $f(x) = (1/2\pi x)\exp(-\frac{1}{2}x)$. If one forms the ratio

$$\frac{\sum_{\langle\Gamma_n^0\rangle/4}^{\infty} \Gamma_n^0}{\left(\sum_{\langle\Gamma_n^0\rangle/4}^{\infty} \sqrt{\Gamma_n^0}\right)^2}\,,$$

it has the expectation value

$$\frac{0.969}{0.704}\,\frac{0.617}{n} = 1.206/n\,,$$

where n is the number of levels having Γ_n^0 larger than $\langle\Gamma_n^0\rangle/4$. To use the missing-level estimator, one calculates the quantity $n\sum\Gamma_n^0/(\sum\sqrt{\Gamma_n^0})^2$, starting with the largest value of Γ_n^0 in the interval and adding additional levels, one at a time, going from larger to smaller values in the ordered array of observed values of Γ_n^0. When this quantity equals 1.206, the total number of levels in the interval is $n/0.617$. The missing-level estimator was tested by Monte Carlo sampling from a Porter-Thomas distribution, and it was found that the expected relative error varies as $1/\sqrt{N}$, where N is the total number of levels in the sample, or ~8.5% for 140 levels. The first attempts[36] to apply the

missing-level estimator to (^{235}U+n) were carried out with four different independent sets of recommended reduced neutron widths for ^{235}U, those of Smith and Young,[29] those of Reynolds,[34] those of de Saussure *et al.*,[31] and those of Mughabghab and Garber,[17] which for the most part are those of Blons.[15] The results are 117± 10, 110± 10, 110 ± 10, and 107± 10, respectively, as the total number of levels below 62 eV. However, when one uses the recommended set of neutron widths listed in Table IV, one obtains a significantly larger value for the estimated total number of levels in this energy range: 139± 12. The reason for this discrepancy is that the estimator is sensitive primarily to the magnitude and number of large neutron widths, and it so happens that several of the large neutron widths obtained in earlier work are actually doublets of mixed spin. The estimate of 139± 12 is expected to be the most reliable.

From a calculation based on the average parameters of Table V, we concluded that the probability that any of the observed resonances below 62 eV are p wave is negligibly small. The results of this calculation also indicate that a few of the s-wave resonances (approaching 20% at 60 eV or 10–12% on the average) may be too small to be observed, and that the probability that such resonances are missed is slightly higher for spin 3 than for spin 4, because the spin-3 resonances have larger average fission widths.

As a result of multilevel interference in fission, the above estimate of 10 to 12% for the number of missing levels below 62 eV may very well be too high. As is well known,[37] a fission resonance having a neutron width with a value of zero is readily observable if it interferes strongly with one or more adjacent resonances. Perhaps the best example of this phenomenon in (^{235}U+n) is the 2.8-eV resonance, for which the parameters obtained by Reynolds[34] or by de Saussure *et al.*[31] would give a peak fission cross section well below 1 b if used in a single-level calculation. The 2.8 eV resonance is readily apparent in the measured data, however, and Figs. 1–5 seem to show several other resonances of this type below 60 eV.

One can also infer that a few levels are still missing by examining the spacing distribution. Figure 14 shows the distribution of observed spacings from the recommended resonance energies listed in Table IV, compared with that calculated from a Wigner distribution of a mixed sequence having the relative densities given by the average parameters in Table V. Although the agreement is markedly superior to any which has been previously observed for (^{235}U+n), the distribution suggests that a few levels are missed.

To obtain the recommended average spacing, we have used the result from the missing-level estimator, that there are 139± 12 levels below 62 eV. Fitting the stairstep curve of a mixed sequence of 139 levels found to be consistent with the Δ_3 statistic gives the recommended average spacing $d=(\langle D_3\rangle^{-1}+\langle D_4\rangle^{-1})^{-1}=0.438\pm 0.038$ eV. The average spacings $\langle D_3\rangle$ and $\langle D_4\rangle$ were obtained by assuming the spin dependence of the level density as

$$\rho\propto(2J+1)\exp[-(J+\tfrac{1}{2})^2/2\sigma^2],$$

with $\sigma\sim 6.5$ in this region of masses,[38,39] leading to the recommended values of 0.953± 0.082 and 0.809± 0.070 eV for the spin-3 and spin-4 spacings, respectively.

The recommended average spacing of 0.438 ± 0.038 eV for levels of both spins is somewhat lower than the 0.53± 0.03 eV obtained by Michaudon *et al.*[20] It is in reasonable agreement with the estimate of 0.38 eV± 10% suggested by Garrison's[40] statistical treatment of missing levels for ^{235}U.

The calculation of the s-wave neutron strength function was done in the usual way, by least-squares fitting of the stairstep curve of $\sum_\lambda \Gamma^0_{\lambda n}$ for resonances having $E_\lambda < E$ as a function of neutron energy below 100 eV. The results give $10^4\langle\Gamma^0_n/D\rangle = 0.945\pm 0.098$ and 1.043 ± 0.089 for spin-3 and spin-4 resonances, respectively, for the parameters listed in Table IV. These parameters pre-

TABLE V. Average parameters for (^{235}U+n) used in the analysis of the unresolved resonance region below 25 keV.

J^π	D (eV)	$S^l=\langle\Gamma^l_n/D\rangle$ ($\times 10^{-4}$)	R^∞	$\langle\Gamma_f\rangle$ (eV)	$\langle\Gamma_\gamma\rangle$ (eV)	ν_f
3^-	0.953 ± 0.082	0.945 ± 0.098	0.0	0.180 ± 0.018	0.035 ± 0.002	3
4^-	0.809 ± 0.070	1.043 ± 0.089	0.0	0.091 ± 0.011	0.035 ± 0.002	2
2^+	1.238	2.25	0.49	0.394	0.035	4
3^+	0.953	a	a	0.227	0.035	3
4^+	0.809	a	a	0.258	0.035	4
5^+	0.748	3.0	0.40	0.179	0.035	3

[a] Neutron strength functions and R^∞ for 3^+ and 4^+ p-wave levels are linear combinations (weighted by the appropriate g factors) of those listed for 2^+ and 5^+ levels.

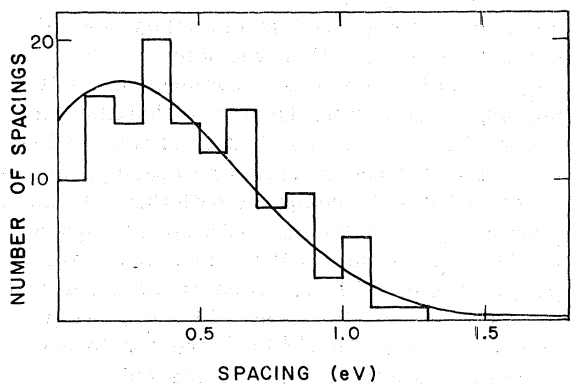

FIG. 14. The resonance spacing distribution for (^{235}U+n) below 62 eV. The histogram shows the spacings obtained from the present work, as listed in Table V; the curve shows the spacing distribution calculated from a Wigner distribution of a mixed sequence having the relative densities recommended in Table VII.

serve the total area $\sigma_0\Gamma$ in broad-bin averages; thus the strength function determination is insensitive to levels that may have been missed.

B. Fission widths

The average fission widths listed in Table V are about a factor of 2 different for the two spin states: $\langle\Gamma_f\rangle_3 = 0.196 \pm 0.012$ eV, $\langle\Gamma_f\rangle_4 = 0.103 \pm 0.007$ eV. However, the determination of the average fission widths by simply averaging the widths as listed for the resolved resonance region may be biased by an experimental problem. The best-known widths are those which are associated with the strong narrow resonances; here the capture-to-fission ratio permits the fission width to be assigned with an accuracy comparable to that assigned to the radiative capture width. The fission widths of the weak levels are poorly known, because one must rely on shape analysis, and generally, they are overestimated because of statistical uncertainties in the data. It is easier to fit the data within the error limits with a resonance shape that is somewhat too wide than with one that is too narrow, and the shape-fitting codes that are commonly used seem to reflect this tendency.

To avoid biasing the determination of the average fission width, an alternate procedure was adopted, one that is similar to the usual method of determining the strength function by least-squares fitting the slope of $\sum_\lambda \Gamma^0_{\lambda n}$ vs E. It may be noted that this method of extracting the strength function is entirely equivalent to fitting the slope of the cumulative sum $\sum_\lambda \sigma_{0\lambda}\Gamma_\lambda\sqrt{E_\lambda}$ vs E, because the quantities are proportional. In the same way, fitting the slope of the cumulative sum $\sum_\lambda \sigma_{0\lambda}\Gamma_{\lambda f}\sqrt{E_\lambda}$ gives the quantity $\langle\Gamma^0_n\Gamma_f/D\Gamma\rangle$, and fitting the slope of the cumulative sum

$$\sum_\lambda \frac{(\sigma_{0\lambda}\Gamma_\lambda - \sigma_{0\lambda}\Gamma_{\lambda f})\sqrt{E_\lambda}\,\Gamma_{\lambda\gamma}}{\Gamma_{\lambda\gamma}+\Gamma_{\lambda n}}$$

gives the quantity $\langle\Gamma^0_n\Gamma_\gamma/D\Gamma\rangle$. This procedure is also similar to that which one uses in calculating average cross sections in the unresolved resonance region, i.e., it gives a result which is weighted according to the neutron strengths of the resonances, and it requires the application of a width fluctuation correction appropriate to the number of fission channels in each spin state before one can arrive at the ratio $\langle\Gamma_f\rangle/\langle\Gamma_\gamma\rangle$. Using the width fluctuation correction procedure of Moldauer[41] and the number of fission channels for each spin, listed in Table V, leads to the recommended average fission widths of 0.180 ± 0.018 eV for spin 3, and 0.091 ± 0.011 eV for spin 4, with the assumption that $\Gamma_\gamma = 0.035$ eV for both spin states, a value chosen on the basis of nuclear systematics.[42]

The only reason one needs to know the number of fission channels or degrees of freedom is to calculate width fluctuation corrections properly. As shown in Table V the number assumed for the analysis of the unresolved resonance region was $\nu_f = 2$ for spin 4, $\nu_f = 3$ for spin 3. Use of somewhat different values does not change the conclusions we reached.

V. VARIATION OF $\langle\Gamma_f\rangle$ BELOW 25 keV

The objective of the unresolved-resonance analysis is the extraction of a self-consistent set of average resonance parameters, $\langle\Gamma_n\rangle$, $\langle\Gamma_f\rangle$, and $\langle\Gamma_\gamma\rangle$, for each s-wave spin state. These average parameters can be energy dependent; they are determined for energy bins which are broad enough to contain a large number of fine-structure (class I) resonances, yet narrow enough to show the effects of possible intermediate structure (class II) states. The data were averaged in bins which ranged from 0.05 keV in width at the lowest energies to 0.5 keV in width near 25 keV. The data were then renormalized to a "best value" of the fission cross section of ^{235}U, averaged over the same bin structure, preserving the ratio of $\langle\sigma_f\rangle_3$ to $\langle\sigma_f\rangle_4$. This was done to remove the effects of resonances, primarily in lanthanum, which were still present in the polarization data. In the preliminary analysis, the "best-value" fission and capture cross sections used were those of Gwin *et al.*[10]; in the final analysis, the "best-value" data were those obtained by Bhat.[43] Figure 15 shows the averaged absorption, fission, spin-separated fission, and radiative capture cross sections

(multiplied by the square root of the neutron energy), and $\langle\alpha\rangle$, the average-radiative-capture to average-fission ratio, as a function of neutron energy from 0.1 to 30 keV. The statistical uncertainties of the spin-separated fission cross sections are shown by the shaded regions on these curves.

The next step in the analysis was the correction of the data shown in Fig. 15 for the p-wave contributions. Most of the cross section at energies below 25 keV is due to s-wave neutron interactions, and the assumption was made that the p-wave interactions can be adequately treated as a correction that is smoothly varying with energy. The p-wave average parameters used for this correction are listed in Table V. The p-wave fission widths and number of degrees of freedom ν_f were chosen by requiring that they give a reasonable fit to the capture-to-fission ratio of Gwin *et al.*[10] at 150 keV. All the data shown in Fig. 15 were then corrected for p-wave contributions; the correction for the spin-separated fission cross sections also requires the use of p-wave polarization factors that are not the same for the two s-wave spin states. The treatment of width fluctuations, both for the p-wave neutron corrections and for the extraction of s-wave average parameters, followed the formalism of Moldauer.[41]

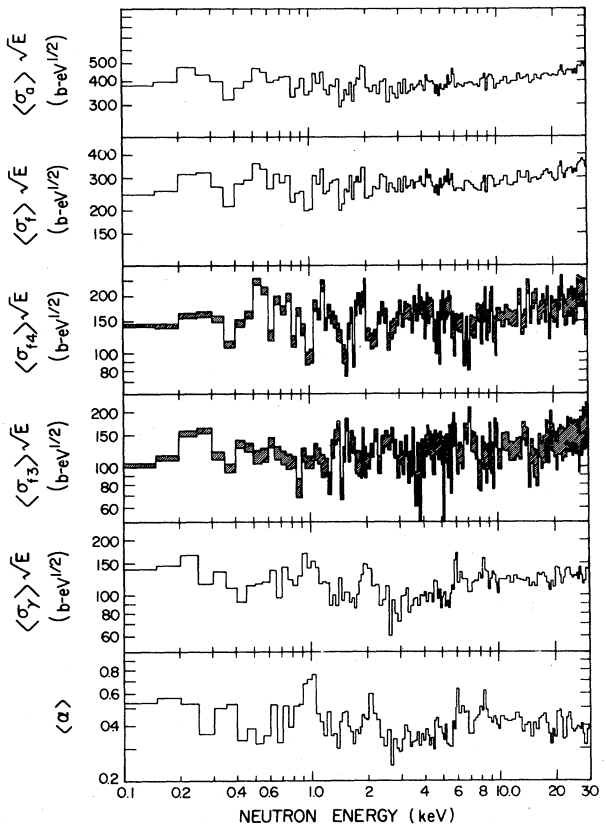

FIG. 15. Partial cross sections and $\langle\alpha\rangle$, the average capture-to-fission ratio for (^{235}U+n) from 0.1 to 30 keV, from Ref. 43. The spin-separated fission cross sections shown in the middle two curves were obtained by renormalizing in each bin such that the sum gives the recommended fission cross section.

At the conclusion of this preliminary data manipulation, there were three sets of data: the spin-3 s-wave fission cross section, the spin-4 s-wave fission cross section, and the s-wave absorption cross section corresponding to the sum of the spin-3 and spin-4 components. If spin-separated absorption cross sections had been available, the analysis would have been almost trivial. In this energy range, the average absorption cross section varies almost linearly with the average neutron width, but varies only very weakly with the average fission width. Thus, the spin-separated absorption cross sections, had they been available, could have been used to extract the average neutron width for each spin state; the neutron widths could then have been used to extract average fission widths consistent with the spin-separated fission cross sections; and, after a few iterations, the problem would have been solved.

Spin-separated absorption cross sections were not measured in this experiment. To carry out the analysis, we were forced to resort to assumptions and self-consistency arguments. Energy bin widths of 0.1 keV are large enough to contain about 100 resonances of each spin state, so that the Porter-Thomas fluctuations in the average neutron widths, while not negligible, are not extremely large (~15%). If there were no intermediate structure in fission, the fluctuations in the average fission widths should also be relatively small. There are thus four average parameters which might fluctuate: $\langle\Gamma_f\rangle_3$, $\langle\Gamma_f\rangle_4$, $\langle\Gamma_n^0\rangle_3$, and $\langle\Gamma_n^0\rangle_4$. However, the three pieces of data available do not allow all four of these to be determined. As limiting cases, we held each of these parameters constant for all bins and solved for the other three as energy-dependent parameters. We then averaged the four sets obtained. The average of the four sets of four parameters will not necessarily describe the data, so a fifth calculation was then made which uses these averaged values as initial guesses and varies each of the parameters in turn by a small increment to obtain the final solution.

The purpose of this study was to test the null hypothesis that there is no evidence for intermediate structure. We used as the four constant input parameters the resolved resonance averages $\langle\Gamma_f\rangle_3 = 0.180$ eV, $\langle\Gamma_f\rangle_4 = 0.091$ eV, $S_3^0 = \langle\Gamma_n^0/D\rangle_3 = 1.043 \times 10^{-4}$, and $S_4^0 = 0.954 \times 10^{-4}$. We found that the data

TABLE VI. Spin-dependent neutron strength functions and average fission widths below 25 keV. The asterisk denotes convergence failure when the resolved-resonance averages are used as the initial guess parameter in the calculation.

Energy (keV)	S_3^0 ($\times 10^{-4}$)	S_4^0 ($\times 10^{-4}$)	$\langle\Gamma_f\rangle_3$ (eV)	$\langle\Gamma_f\rangle_4$ (eV)	Energy (keV)	S_3^0 ($\times 10^{-4}$)	S_4^0 ($\times 10^{-4}$)	$\langle\Gamma_f\rangle_3$ (eV)	$\langle\Gamma_f\rangle_4$ (eV)
0.0– 0.1	0.945	1.043	0.180	0.091	6.0– 6.5	0.836	1.059	0.131	0.106
0.1– 0.2	0.889	1.070	0.129	0.096	6.5– 7.0	0.965	0.937	0.227	0.084
0.2– 0.3	1.154	1.182	0.211	0.107	7.0– 7.5	1.088	0.871*	0.261	0.084
0.3– 0.4	0.828	0.989	0.166	0.100	7.5– 8.0	0.818	1.068	0.119	0.110
0.4– 0.5	0.914	1.019	0.281	0.148*	8.0– 8.5	0.886	1.130	0.088	0.094
0.5– 0.6	0.935	1.372*	0.138	0.266*	8.5– 9.0	0.809	1.125	0.115	0.127
0.6– 0.7	0.933	1.104	0.218	0.130	9.0– 9.5	0.944	1.192	0.136	0.126
0.7– 0.8	0.917	1.244	0.125	0.153	9.5–10.0	0.892	0.980	0.202	0.101
0.8– 0.9	0.758	1.012	0.125	0.114	10.0–10.5	0.772	1.066	0.106	0.123
0.9– 1.0	0.967	1.002	0.111	0.064	10.5–11.0	0.896	1.041	0.168	0.102
1.0– 1.1	0.961	1.100	0.123	0.086	11.0–11.5	0.924	1.125	0.147	0.113
1.1– 1.2	0.911	1.223	0.124	0.216*	11.5–12.0	0.775	1.019	0.136	0.114
1.2– 1.3	0.720	1.021	0.140	0.165*	12.0–12.5	0.823	1.039	0.112	0.099
1.3– 1.4	0.935	0.979	0.285	0.163*	12.5–13.0	0.815	1.011	0.136	0.104
1.4– 1.5	0.865	0.932	0.219	0.105	13.0–13.5	0.851	1.210	0.109	0.180*
1.5– 1.6	1.022	0.736*	0.254	0.080	13.5–14.0	0.953	0.949	0.209	0.089
1.6– 1.7	0.895	0.960	0.279	0.157*	14.0–14.5	0.900	1.013	0.168	0.096
1.7– 1.8	0.842	0.899*	0.239	0.146*	14.5–15.0	0.645*	1.219*	0.059	0.288*
1.8– 1.9	0.883	1.228	0.116	0.171*	15.0–15.5	0.721	0.971	0.120	0.119
1.9– 2.0	1.105	1.448	0.114	0.163	15.5–16.0	0.626	1.082	0.082	0.183*
2.0– 2.2	0.889	0.966	0.158	0.082	16.0–16.5	0.677	1.206	0.048	0.167
2.2– 2.4	0.874	0.959	0.259	0.125	16.5–17.0	0.814	1.014	0.110	0.100
2.4– 2.6	0.964	1.090	0.252	0.164*	17.0–17.5	0.724	1.059	0.078	0.112
2.6– 2.8	0.953	0.758*	0.317	0.182*	17.5–18.0	0.757	1.108	0.097	0.138
2.8– 3.0	0.791	0.841*	0.212	0.254*	18.0–18.5	0.865	0.999	0.204	0.114
3.0– 3.2	0.806	1.037	0.187	0.172*	18.5–19.0	0.697	1.072	0.117	0.229*
3.2– 3.4	0.820	1.046	0.189	0.200*	19.0–19.5	0.981	0.845	0.230	0.080
3.4– 3.6	0.851	0.982	0.254	0.173*	19.5–20.0	0.740	0.983	0.164	0.144
3.6– 3.8	0.739	1.034	0.134	0.244*	20.0–20.5	0.844	1.052	0.081	0.091
3.8– 4.0	0.775	1.147	0.103	0.280*	20.5–21.0	0.708	1.053	0.059	0.100
4.0– 4.2	0.810	1.003	0 214	0.150*	21.0–21.5	0.768	0.927	0.102	0.094
4.2– 4.4	0.973	1.113	0.230	0.180*	21.5–22.0	0.744	1.069	0.130	0.177*
4.4– 4.6	0.866	1.116	0.169	0.180*	22.0–22.5	0.784	1.257*	0.080	0.226*
4.6– 4.8	0.921	0.907	0.244	0.095	22.5–23.0	0.773	1.073	0.086	0.106
4.8– 5.0	0.879	0.857*	0.256	0.117	23.0–23.5	0.784	0.968	0.080	0.086
5.0– 5.2	0.742	1.097	0.103	0.231*	23.5–24.0	0.916	1.008	0.119	0.088
5.2– 5.4	0.845	0.970	0.232	0.193*	24.0–24.5	0.769	1.061	0.108	0.135
5.4– 5.6	0.864	1.079	0.195	0.233*	24.5–25.0	0.785	0.996	0.139	0.121
5.6– 5.8	0.843	1.077	0.179	0.138					
5.8– 6.0	1.362	1.124	0.129	0.065					

are not always consistent with these initial values for certain of the parameters. In particular, about one-third of the calculations failed to give a solution with $\langle\Gamma_f\rangle_4$ set equal to 0.091 eV. The reason for this is not difficult to see: One can easily find a value of the neutron strength function S_4^0 which is consistent with the spin-4 fission cross section as measured, and with $\langle\Gamma_f\rangle_4 = 0.091$ eV. One then calculates a spin-4 absorption cross section and subtracts it from the measured s-wave absorption cross section to get the spin-3 absorption cross section. If this quantity is less than the measured spin-3 fission cross section, then no solution with nonnegative widths is possible, and the iterative procedure used in the calculation cannot converge.

The asterisks in Table VI summarize the energy dependence of such convergence failures for each of the input parameters. The rate of convergence failure for $\langle\Gamma_f\rangle_4 = 0.091$ eV shows clearly a nonrandom behavior, consistent with the statistical tests indicating the presence of intermediate

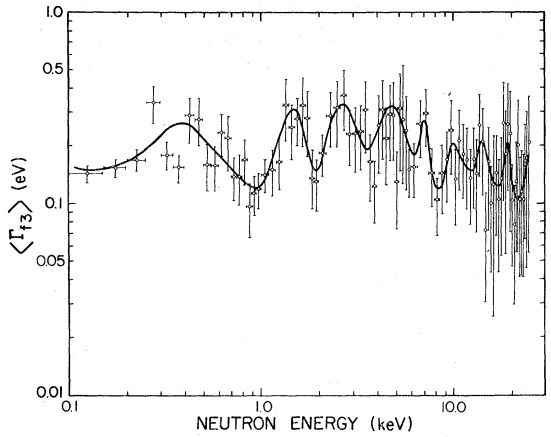

FIG. 16. Average spin-3 fission width for (^{235}U+n) from 0.1 to 25 keV obtained from the unresolved resonance analysis described in the text. The curve has no theoretical significance; it is simply the authors' eyeguide.

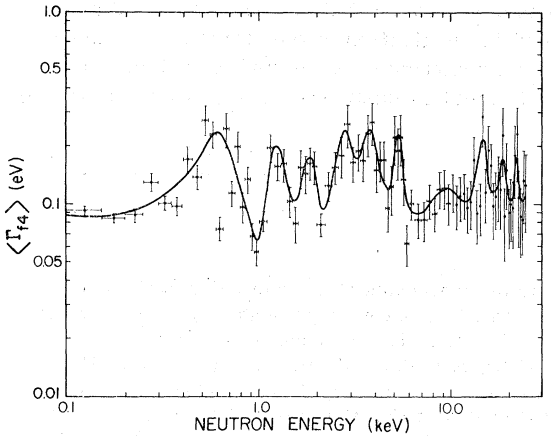

FIG. 17. Average spin-4 fission width for (^{235}U+n) from 0.1 to 25 keV obtained from the unresolved resonance analysis described in the text. The curve has no theoretical significance; it is simply the authors' eyeguide.

structure in (^{235}U+n) in this region.[1-4] It also may be noted that the initial guess that $\langle\Gamma_f\rangle_3$ is constant and equal to 0.180 eV never fails to give a reasonable solution for the other three parameters.

To complete these studies, we allowed $\langle\Gamma_f\rangle_4$, or any of the parameters that failed to give a solution, to vary by one standard deviation from the resolved-resonance average, repeating this until a solution consistent with the data could be found. The resulting average fission widths and neutron strength functions obtained are listed in Table VI and the fission widths are plotted in Figs. 16 and 17. The uncertainties in Figs. 16 and 17 are those which arise from the statistical uncertainties in the spin-separated fission cross sections; the smooth curves are eye guides drawn to show the significant structure.

No uncertainties are listed in Table VI. The set of values shown is only one of many that could be obtained; in particular, it is the one which is most nearly consistent with the resolved-resonance averages. The four solutions that were averaged to obtain the results shown in Table VI have one striking common feature: They all reproduce the structure in $\langle\Gamma_f\rangle_4$ shown in Fig. 17. This is true even for the solution in which $\langle\Gamma_f\rangle_4$ was set equal to 0.091 eV; the convergence failures force $\langle\Gamma_f\rangle_4$ above the value and qualitatively describe the structure.

Other solutions were also investigated, with somewhat different constraints. All the solutions studied have the same common feature: The relative fluctuations in the four parameters listed in Table VI are reproduced, although the magnitudes are different.

The results of these studies can be summarized as follows: The data are clearly not consistent with a constant value of $\langle\Gamma_f\rangle_4$ as inferred from the resolved resonances, or with the small variation (~10–15%) expected from Porter-Thomas fluctuations in two or three open fission channels. If $\langle\Gamma_f\rangle_4$ is allowed to vary, then its variation is found to be qualitatively consistent with that shown in Fig. 17. The fluctuations in $\langle\Gamma_f\rangle_4$ are not small and not randomly distributed, and they are quite consistent with the conclusions reached, for example, by Migneco *et al.*[3] in their study of intermediate structure in ^{235}U fission: The average spacing is between 0.5 and 1.0 keV, and the effects are readily seen with bin widths of 100 to 500 eV. Figure 16 is strongly suggestive that intermediate structure is also present in the spin-3 component. It must be emphasized, however, that the data can also be interpreted as being consistent with the assumption that the spin-3 average fission widths are nearly constant, with an average value given by that observed for the resolved resonances. The present work definitely confirms the existence of intermediate structure in the fission widths only for the spin-4 component.

ACKNOWLEDGMENTS

The authors would like to acknowledge several helpful discussions with, and useful suggestions made by, J. E. Lynn and R. L. Macklin during the data analysis. We are especially grateful to R. Gwin for supplying the results of his capture and fission cross-section measurements in fine bin averages, which made the preliminary analysis of the unresolved resonance region possible.

Thanks are also due M. R. Bhat for providing results of his evaluation of the structure in the unresolved resonance region, and A. Prince for the optical model calculations we used to obtain initial guesses for the p-wave strength functions. This work was performed under the auspices of the United States Energy Research and Development Administration.

---

*Preliminary accounts of some of the material contained in this paper were presented by G. A. Keyworth, M. S. Moore, and J. D. Moses at the NEANDC/NEACRP Specialists' Meeting on Fast Neutron Fission Cross Sections of U-233, U-235, U-238, and Pu-239, USERDA Report No. ANL-76-90, 1976 (unpublished), p. 353 and by G. A. Keyworth at the International Conference on the International Conference on the Interaction of Neutrons by Nuclei, Lowell, Massachusetts, USERDA Report No. CONF-760715-P1, 1976 (unpublished).

[1]M. G. Cao, E. Migneco, and J. P. Theobald, Phys. Lett. 27B, 409 (1968).

[2]R. B. Perez, G. de Saussure, E. G. Silver, R. W. Ingle, and H. Weaver, Nucl. Sci. Eng. 55, 203 (1974).

[3]G. D. James, G. de Saussure, and R. B. Perez, Trans. Am. Nucl. Soc. 17, 495 (1973); see also UKNDC (74) P63, p. 38, 1974 (unpublished).

[4]E. Migneco, P. Bonsignore, G. Lanzano, J. A. Wartena, and H. Weigmann, Nuclear Cross Sections and Technology, NBS Special Publication No. 425, 1975 (unpublished), Vol. II, p. 607.

[5]G. A. Keyworth, J. R. Lemley, C. E. Olsen, F. T. Seibel, J. W. T. Dabbs, and N. W. Hill, Phys. Rev. C 8, 2362 (1973).

[6]G. A. Keyworth, J. R. Lemley, C. E. Olsen, F. T. Seibel, J. W. T. Dabbs, and N. W. Hill, *Physics and Chemistry of Fission 1973* (IAEA, Vienna, 1974), Vol. I, p. 97.

[7]G. A. Keyworth, C. E. Olsen, F. T. Seibel, J. W. T. Dabbs, and N. W. Hill, Phys. Rev. Lett. 31, 1077 (1973).

[8]F. L. Shapiro, in *Nuclear Structure Study with Neutrons*, edited by M. Nève de Mévergnies, P. Van Assche, and J. Vervier (North-Holland, Amsterdam, 1966), p. 223.

[9]B. R. Leonard, Jr., in Proceedings of the NEANDC/NEACRP Specialists Meeting on Fast Neutron Fission Cross Sections of U-233, U-235, U-238, and Pu-239, edited by W. P. Poenitz and A. B. Smith [ANL Report No. ANL-76-90, 1976 (unpublished)], p. 281.

[10]R. Gwin, E. G. Silver, R. W. Ingle, and H. Weaver, Nucl. Sci. Eng. 59, 79 (1976). We are especially indebeted to Dr. Gwin for providing fine-bin-averaged absorption and fission cross-section data to be used in this analysis.

[11]H. E. Liou, G. Hacken, F. Rahn, J. Rainwater, M. Slagowitz, and W. Makofske, Phys. Rev. C 10, 709 (1974).

[12]G. M. Hale, in Nuclear Cross Sections and Technology, NBS Special Publication No. 425, 1975 (unpublished), Vol. I, p. 302; private communication.

[13]F. J. Shore and V. I. Sailor, Phys. Rev. 112, 191 (1958).

[14]R. I. Schermer, L. Passell, G. Brunhart, C. A. Reynolds, V. L. Sailor, and F. J. Shore, Phys. Rev. 167, 1121 (1968).

[15]J. Blons, Nucl. Sci. Eng. 51, 130 (1973); J. Blons, H. Derrien, and A. Michaudon, in Neutron Cross Sections and Technology, USAEC Proceedings CONF-710301, 1971 (unpublished), Vol. 2, p. 829.

[16]E. R. Reddingius, H. Postma, C. E. Olsen. D. C. Rorer, and V. L. Sailor, Nucl. Phys. A218, 84 (1974).

[17]*Neutron Cross Sections*, by S. Mughabghab and D. I. Garber, Brookhaven National Laboratory Report No. BNL-325 (National Technical Information Service, Springfield, Virginia, 1973), 3rd ed., Vol. I.

[18]F. J. Dyson and M. L. Mehta, J. Math. Phys. 4, 703 (1963).

[19]F. J. Dyson, as described by M. L. Mehta in *Statistical Properties of Nuclei*, edited by J. B. Garg (Plenum, New York, 1972), p. 179.

[20]A. Michaudon, H. Derrien, P. Ribon, and M. Sanche, Nucl. Phys. 69, 545 (1965).

[21]Wang Shih-Ti, Wang Yun-Chang, E. Dermendzhiev, and Yu. V. Ryabov, in *Physics and Chemistry of Fission* (IAEA, Vienna (1965), Vol. I, p. 287; see also Atom. Energ. 19, 43 (1965) [Sov. J. Atom. Energ. 19, 907 (1965)]; Dubna Report No. JINR-P3-4992, 1970 (unpublished).

[22]D. W. Drawbaugh and G. Gibson, in *Nuclear Data for Reactors* (IAEA, Vienna, 1967), Vol. II, p. 251; see also USAEC Reports Nos. WANL-TME-1596, 1967 and WANL-TME-2705, 1970 (unpublished).

[23]G. de Saussure, R. Gwin, L. W. Weston, R. W. Ingle, and H. Weaver, in *Nuclear Data for Reactors* (IAEA, Vienna, 1967), Vol. II, p. 233; USAEC Report No. ORNL-TM-1804, 1967 (unpublished).

[24]D. B. Adler and F. T. Adler, USAEC Report No. BNL-50045 (T-455), 1967 (unpublished).

[25]M. G. Cao, E. Migneco, J. P. Theobald, J. A. Wartena, and J. Winter, J. Nucl. Energy 22, 211 (1968).

[26]J. D. Cramer, Nucl. Phys. A126, 471 (1969).

[27]G. de Saussure, R. B. Perez, and H. Derrien, in *Nuclear Data for Reactors* (IAEA, Vienna, 1970), Vol. II, p. 757.

[28]J. Krebs, G. le Coq, J. P. l'Heriteau, and P. Ribon, in Neutron Cross Sections and Technology, USAEC Proceedings No. CONF-710301, 1971 (unpublished), Vol. 1, p. 410.

[29]J. R. Smith and R. C. Young, USAEC Report No. ANCR-1044, 1971 (unpublished); J. R. Smith, USAEC Report No. ANCR-1129, 1973 (unpublished), p. 10.

[30]J. P. Felvinci and E. Melkonian, Trans. Am. Nucl. Soc. 15, 944 (1972).

[31]G. de Saussure, R. B. Perez, and W. Kolar, Phys. Rev. C 7, 2018 (1973).

[32]R. B. Perez, G. de Saussure, E. G. Silver, R. W. Ingle, and H. Weaver, Nucl. Sci. Eng. 52, 46 (1973);

USAEC Report No. ORNL-TM-3696, 1972 (unpublished).
[33]V. A. Konshin, G. B. Morogovskij, and E. Sh. Sukhovitskij, IAEA Report No. INDC(CCP)-78/U, 1976 (unpublished), p. 7.
[34]J. T. Reynolds, USAEC Report KAPL-M-7396, 1975 (unpublished); and private communication.
[35]J. B. Garg, W. W. Havens, Jr., and J. Rainwater, as communicated privately to the National Nuclear Data Center at Brookhaven National Laboratory.
[36]G. A. Keyworth, M. S. Moore, and J. D. Moses, in Proceedings of the NEANDC/NEACRP Specialists Meeting on Fast Fission Cross Sections of U-233, U-235, U-238, and Pu-239, edited by W. P. Poenitz and A. B. Smith [ANL Report No. ANL-76-90, 1976 (unpublished), p. 353.]
[37]M. S. Moore and C. W. Reich, Phys. Rev. 118, 718 (1960); see also Bull. Am. Phys. Soc. 5, 294 (1960).
[38]A. Gilbert and A. G. W. Cameron, Can. J. Phys. 43, 1446 (1965).
[39]B. B. Bach, O. Hansen, H. C. Britt, and J. D. Garrett, Phys. Rev. C 9, 1924 (1974).
[40]J. D. Garrison, Phys. Rev. Lett. 29, 1185 (1972).
[41]P. A. Moldauer, Phys. Rev. C 14, 764 (1976).
[42]M. S. Moore, in Proceedings of the International Conference on Neutron Physics and Nuclear Data for Reactors and Other Applied Purposes, Harwell, 1978 (to be published).
[43]M. R. Bhat, private communication.